



# Producing Next Generation Superalloys Through Advanced Characterization and Manufacturing Techniques

Dr. Tim Smith

NASA Glenn Research Center



# Outline

- Part 1: Enhancing the strength of Ni-base Disk Superalloys
  - Turbine Engines
  - Creep Deformation
  - Scanning Transmission Electron Microscopy
  - Phase Transformation Strengthening
- Part 2: Efficient Production of a Dispersion Strengthened Multi-Principal Element Alloy (MPEA)
  - Additive Manufacturing
  - Solid Solution Strengthening
  - Dispersion Strengthening



# Part 1: Enhancing the Creep Strength of Ni-base Superalloys

T.M. Smith<sup>1</sup>, B. Good<sup>1</sup>, T. Gabb<sup>1</sup>, B.D. Esser<sup>2</sup>, A. Egan<sup>2</sup>, C.M.F. Rae<sup>3</sup>,  
L. Evans<sup>1</sup>, A. Leary<sup>1</sup>, D.W McComb<sup>2</sup>, M.J. Mills<sup>2</sup>

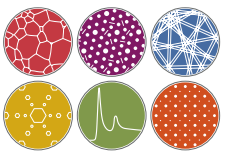
<sup>1</sup>NASA Glenn Research Center, Cleveland Oh 44135 USA

<sup>2</sup>Center for Electron Microscopy and Analysis, The Ohio State University, Columbus Oh 43212 USA

<sup>3</sup> Department of Materials Science and Metallurgy, University of Cambridge, Cambridge CB2 3QZ, UK

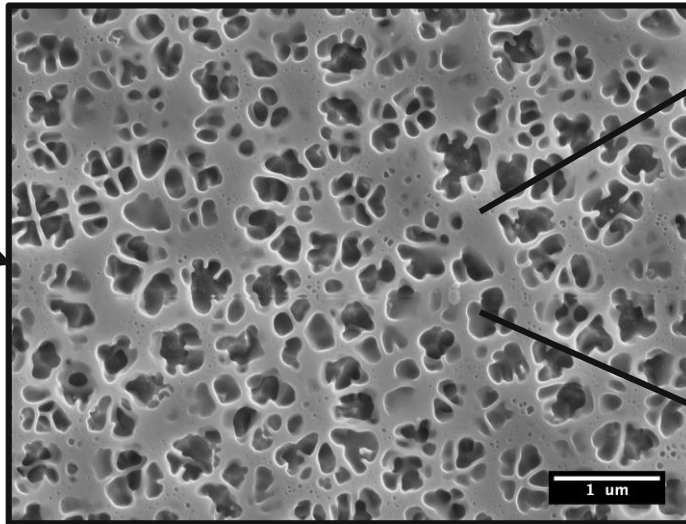
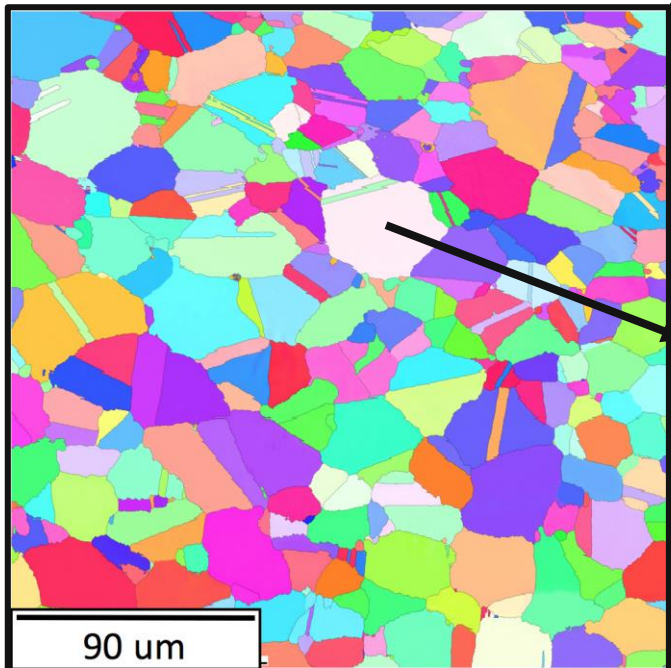
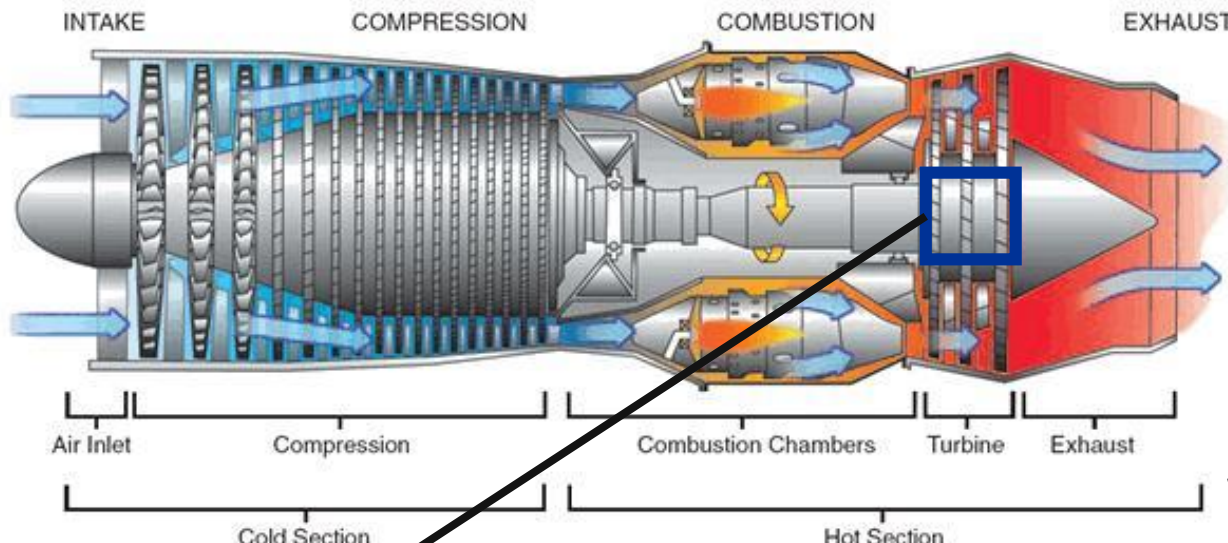


*Support provided by NASA's Aeronautics Research Mission Directorate (ARMD) – Convergent Aeronautics Solutions Project and NASA's Advanced Air Transport Technology (AATT) Project Office (ARMD) and NSF DMREF Program*

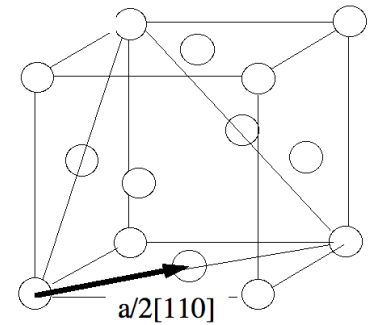


Center for Electron  
Microscopy and Analysis

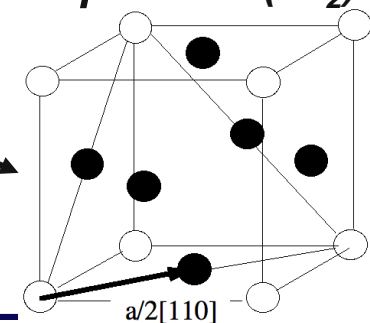
# Ni-Based Superalloys for Turbine Disks



$\gamma$  Phase (FCC)



$\gamma'$  Phase ( $L1_2$ )

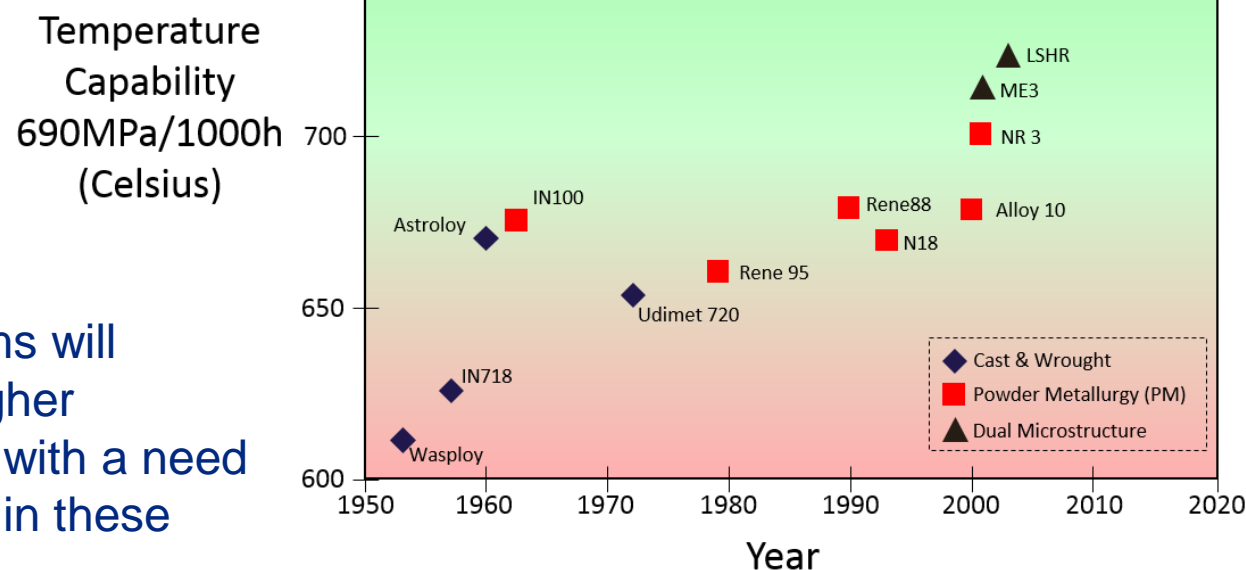




# Motivation for Mechanistic Studies

- Material advancements are required to accommodate the higher compressor exit temperatures in jet turbine engines (>700°C near the rotor rim) for improved efficiency and pollution reduction.

Temperature Capability  
690 MPa/1000h (Celsius)

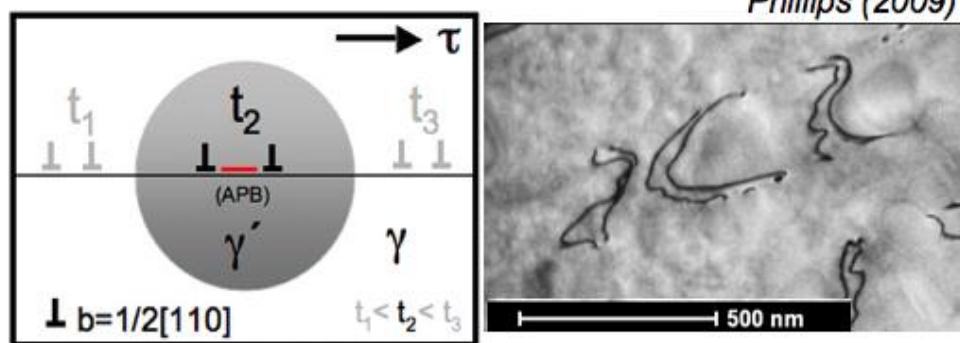


- New deformation mechanisms will become dominant at these higher operating temperatures along with a need for improved creep properties in these disk alloys.

- New understanding and materials will be needed for future advancements

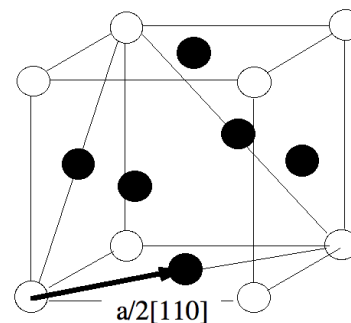
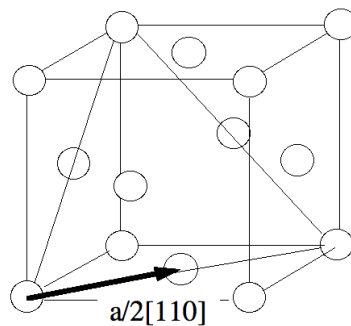
# Deformation Mechanisms in Superalloys

**Disk Alloys**  
 $T < 700^{\circ} \text{ C}$

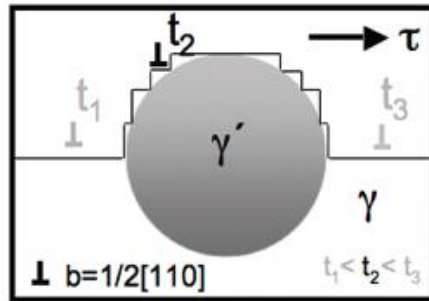
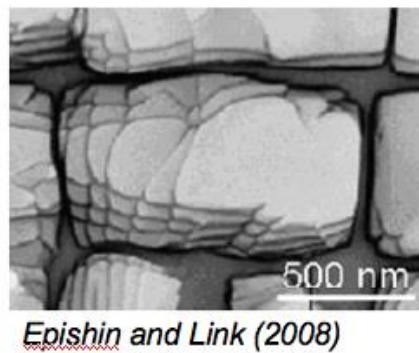


Athermal  $\gamma'$  shearing  
 by  $1/2<110>$   
 dislocations

**$\gamma$  Phase (FCC)**



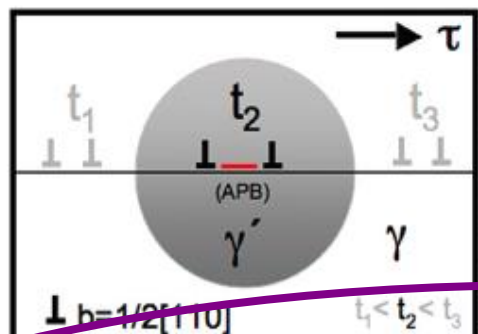
**Blade Alloys**  
 $T > 900^{\circ} \text{ C}$



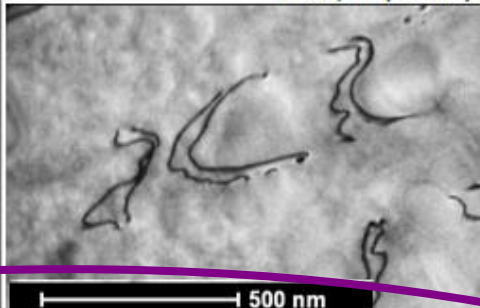
Climb By-Pass  
 of  $\gamma'$  by individual  
 $1/2<110>$   
 dislocations

# Deformation Mechanisms in Superalloys

**Disk Alloys**  
 $T < 700^{\circ} \text{ C}$



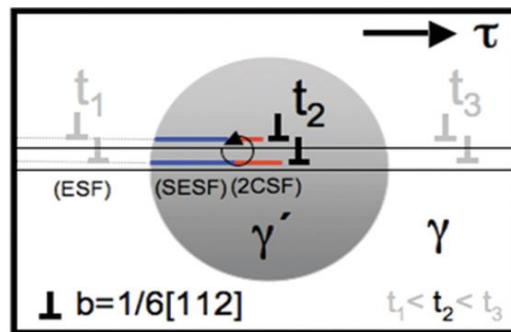
Phillips (2009)



Athermal  $\gamma'$  shearing  
 by  $1/2<110>$   
 dislocations

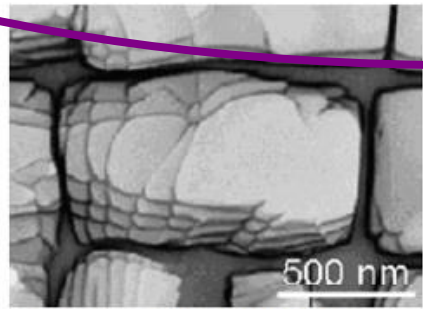
**Novel mechanisms:**  

- Stacking Fault Cutting
- Microtwinning
- Stacking Fault Ribbons

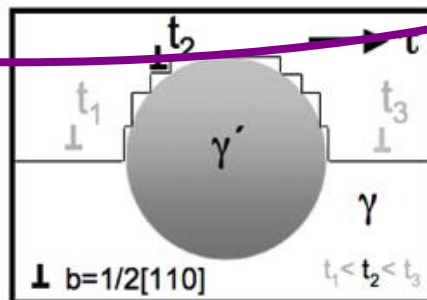


Diffusion mediated creep deformation

**Blade Alloys**  
 $T > 900^{\circ} \text{ C}$



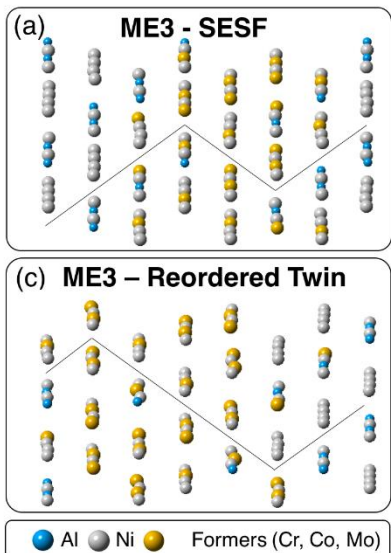
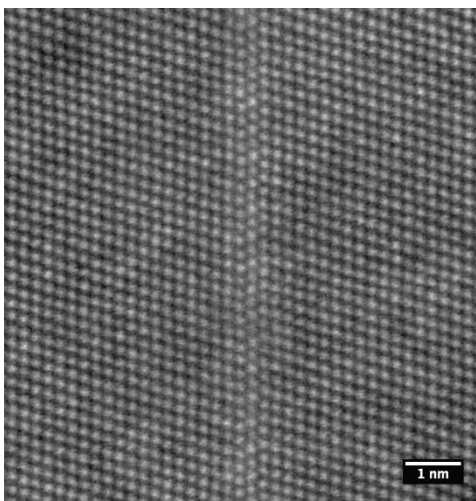
Epishin and Link (2008)



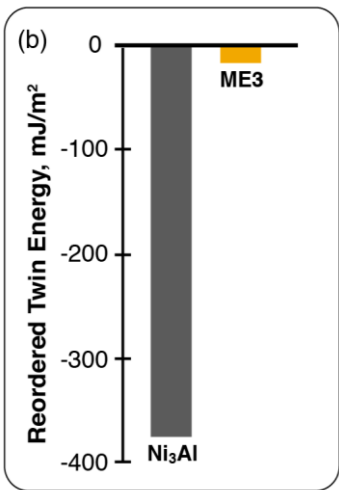
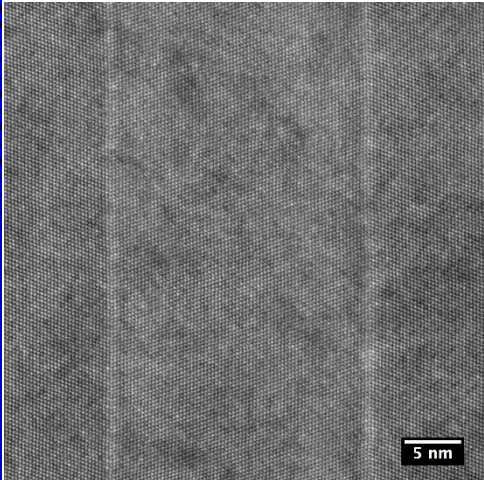
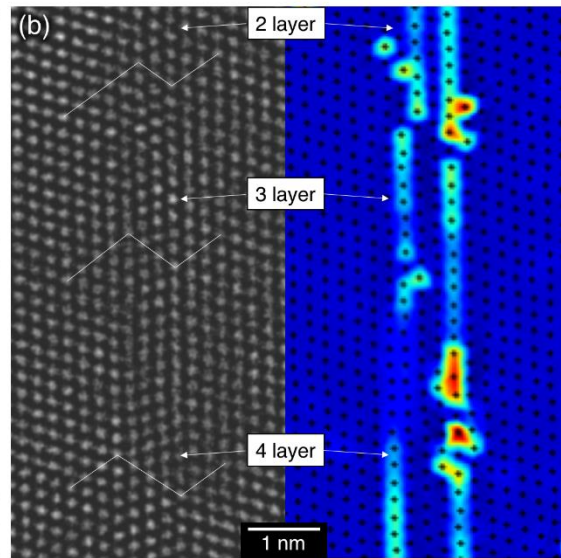
Climb By-Pass of  $\gamma'$  by individual  
 $1/2<110>$   
 dislocations

# Deformation Mechanisms: Microtwinning

SESFs

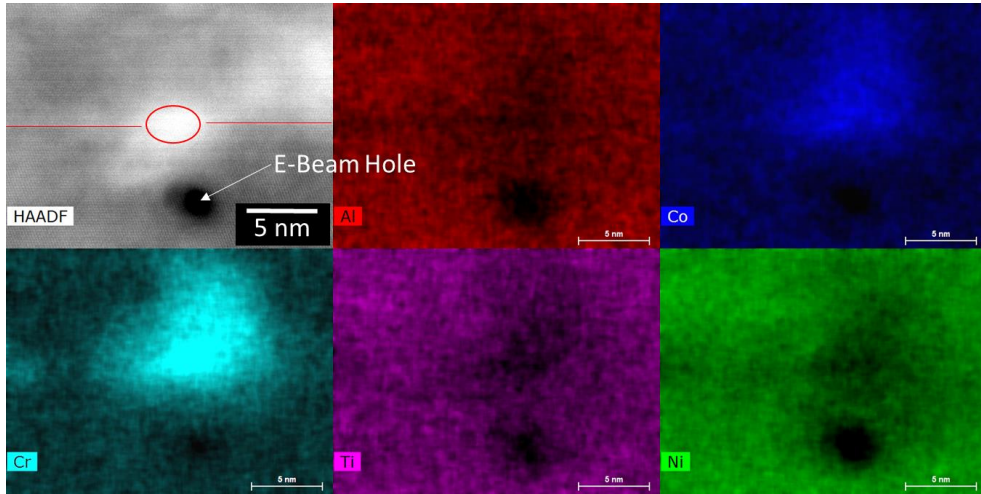
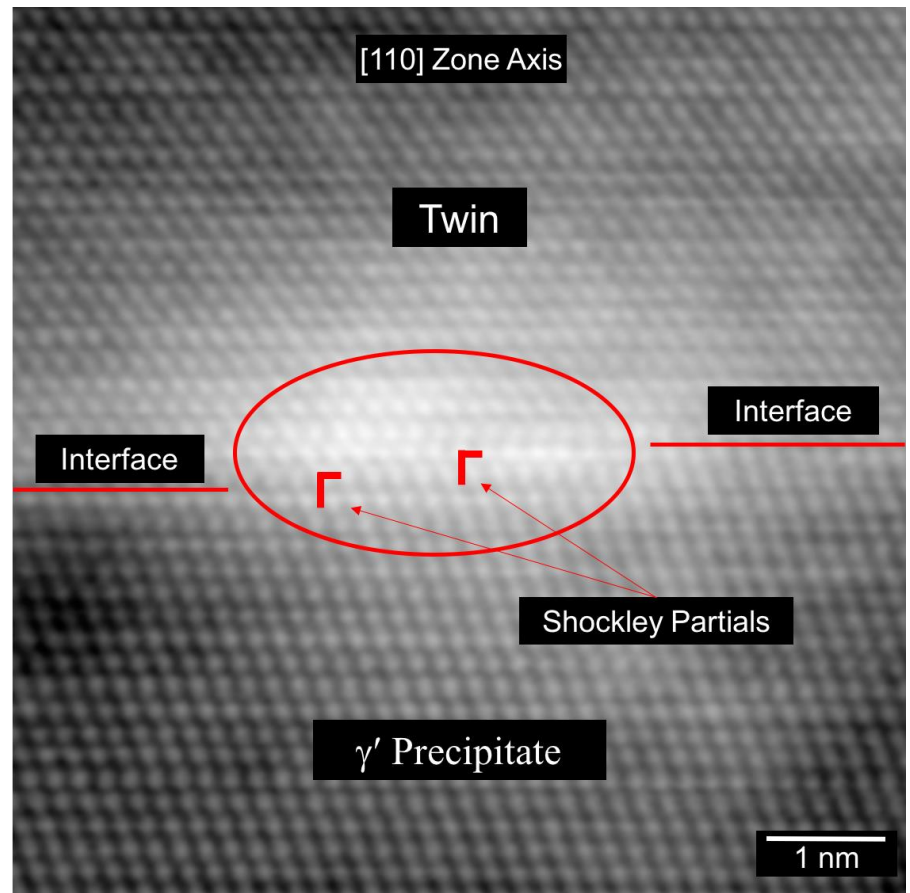


Microtwins



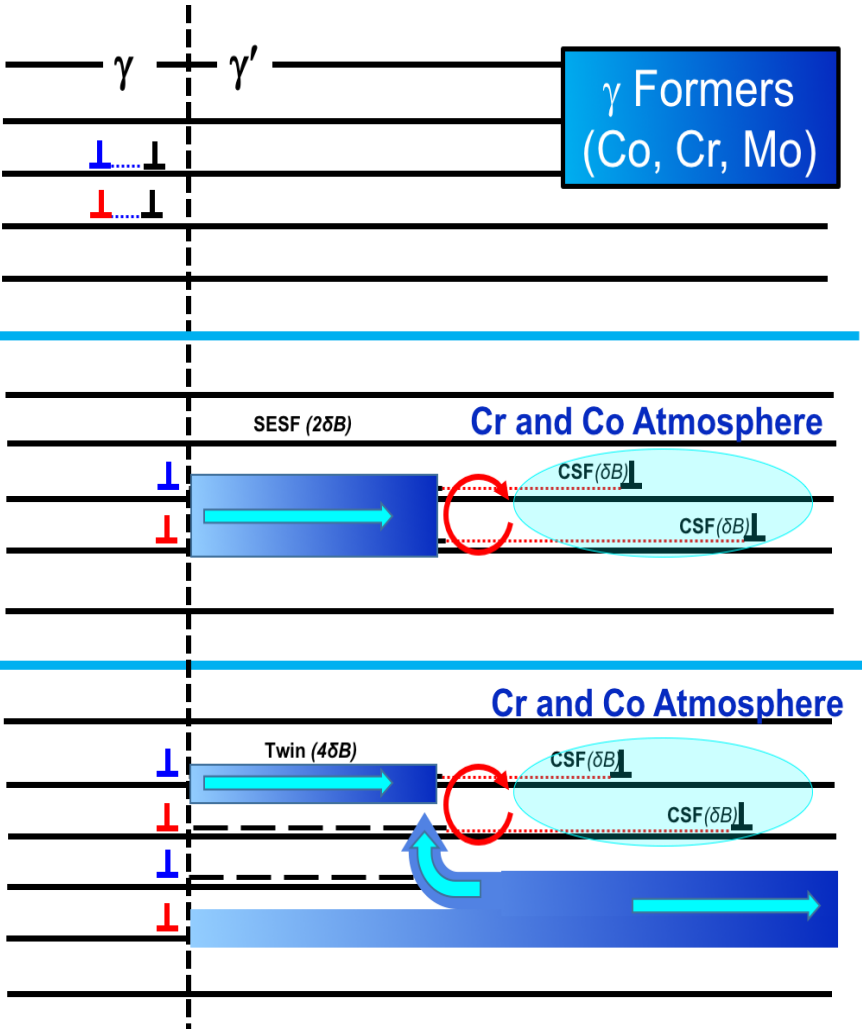
- Microtwins thicken from SESFs via additional Shockley partial pairs shearing along (111) fault planes
- Segregation of “γ former” elements strongly reduces energy penalty for twinning

# Deformation Mechanisms: Microtwinning

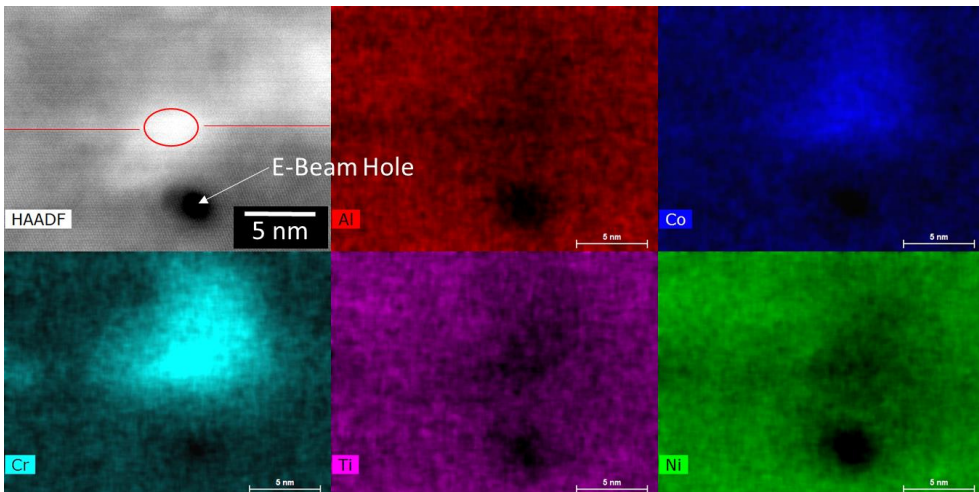


- Dissimilar matrix dislocations react at  $\gamma/\gamma'$  interface – shearing by Shockley partial pairs
- Stacking fault shearing controlled by segregation and Cottrell atmospheres
- Rate of microtwinning also limited by segregation and Cottrell atmospheres
- Can these deformation modes be mitigated/eliminated?

# Deformation Mechanisms: Microtwinning

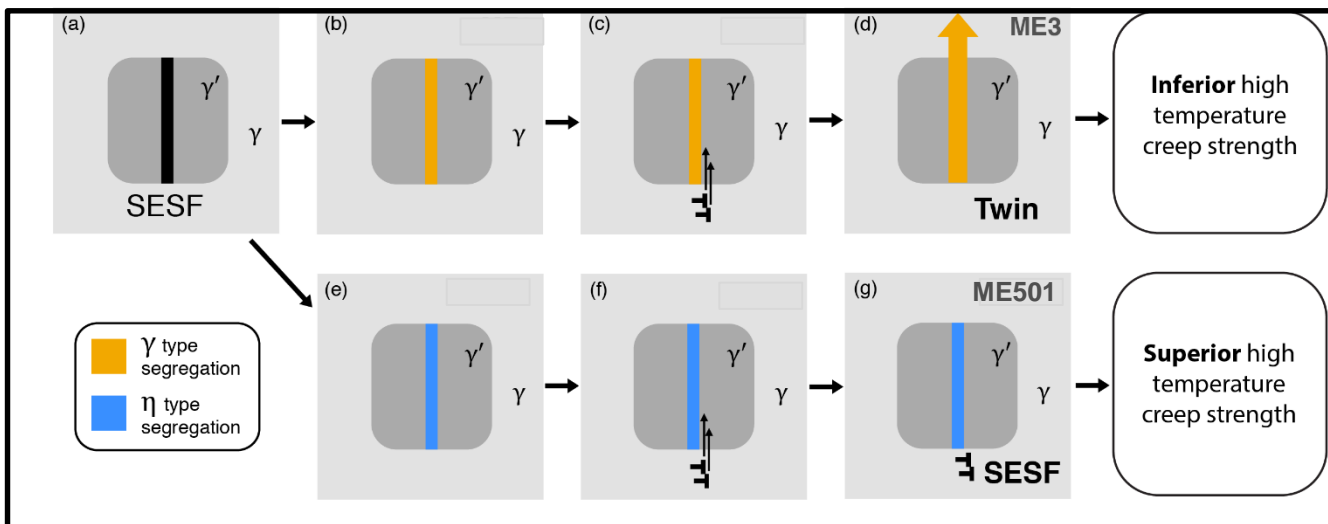
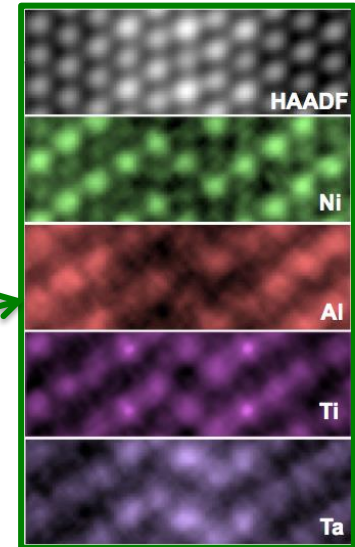
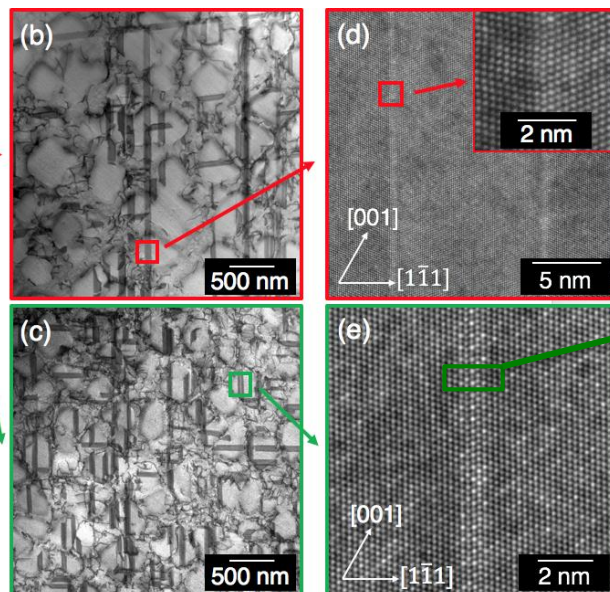
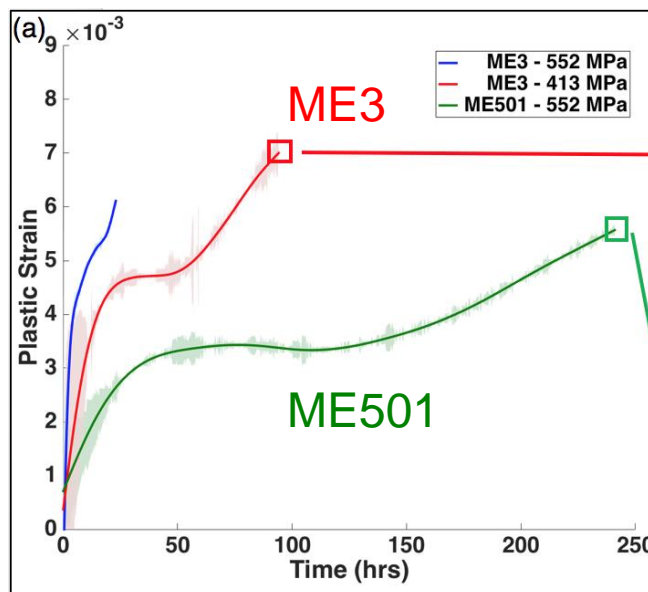


Smith, et al. Acta Materialia, 2017



- Dissimilar matrix dislocations react at  $\gamma/\gamma'$  interface – shearing by Shockley partial pairs
- Stacking fault shearing controlled by segregation and Cottrell atmospheres
- Rate of microtwinning also limited by segregation and Cottrell atmospheres
- Can these deformation modes be mitigated/eliminated?

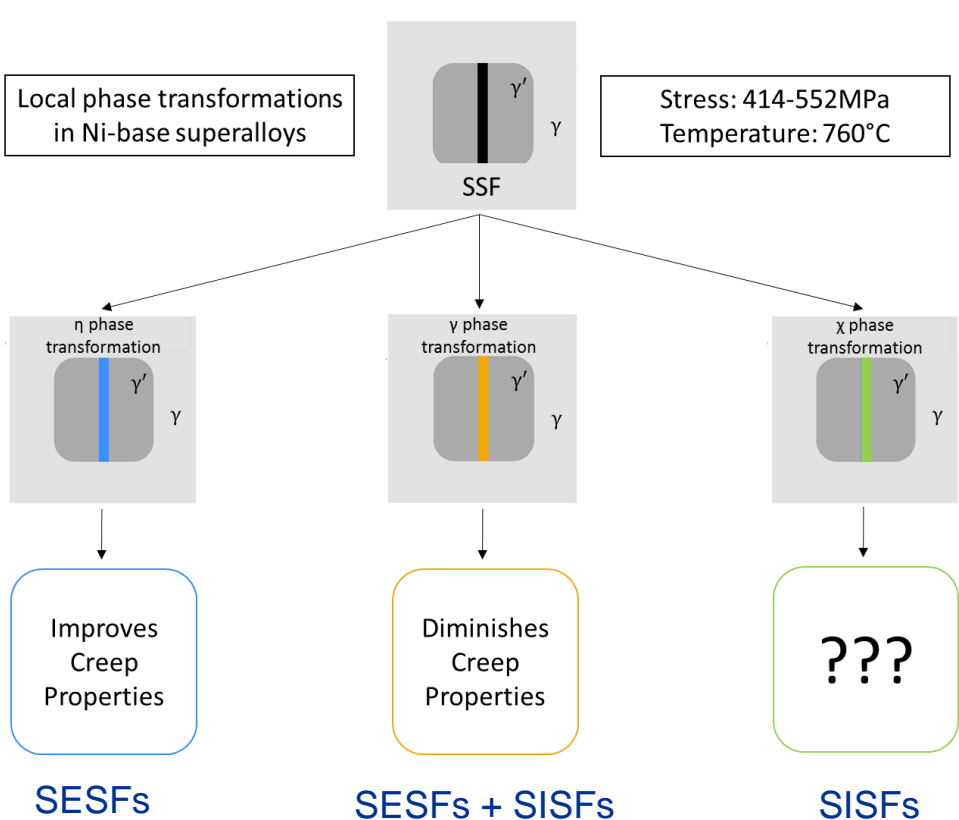
# Phase Transformation Strengthening



## New insight into alloy effects:

- Segregation of  $\gamma$  formers in ME3 promotes microtwinning
- Formation of  $\eta$  phase at faults in ME501 inhibits microtwinning and improves creep strength

# Phase Transformations along SISFs

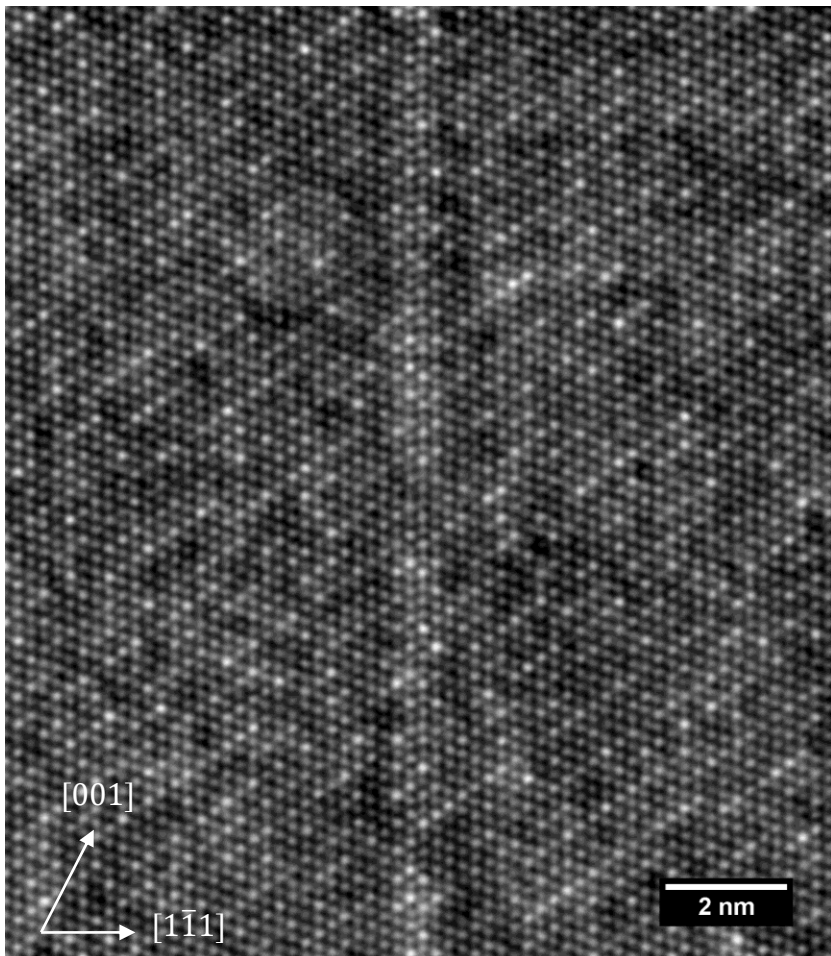


Does the observed  $\chi$  ( $\text{Co}_3\text{W}$ ) or  $\gamma$  phase transformations along SISFs have any impact on creep properties?

\*Smith et al. 2018

SESF = Superlattice Extrinsic Stacking Fault

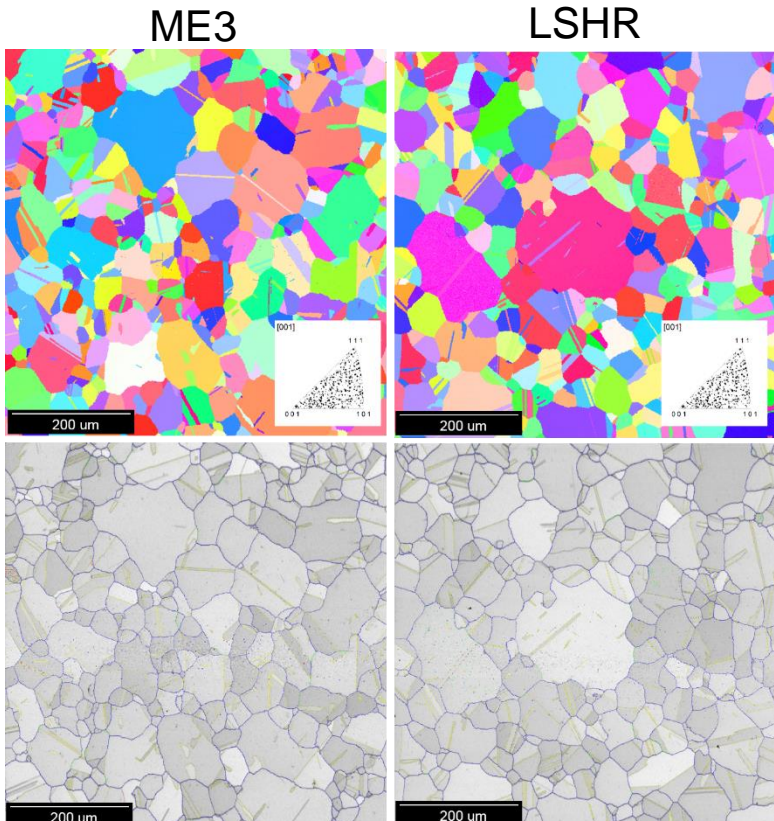
SISF = Superlattice Intrinsic stacking Fault



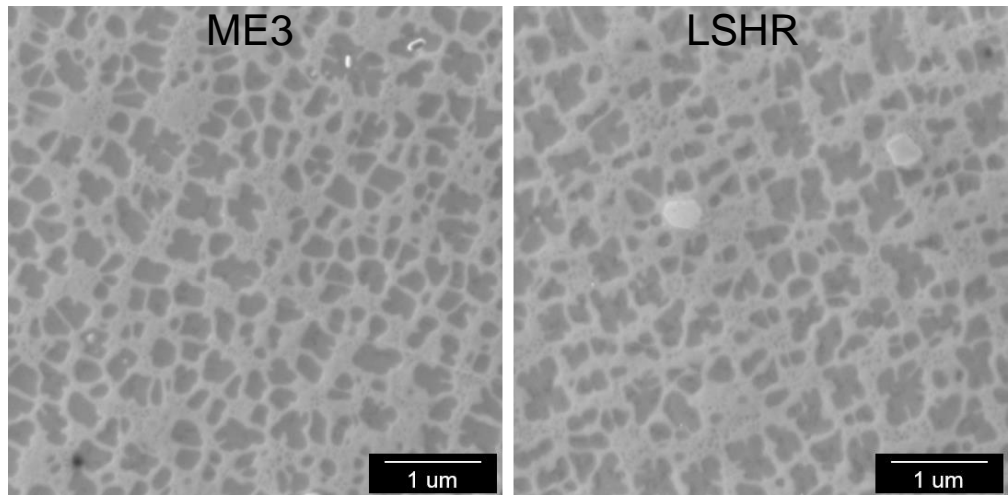
CMSX-4 (high W content)\*

# Material Preparation

Average Alloy Composition in Weight Percent												
Alloy	Cr	Co	Al	Ti	Nb	Mo	Ta	W	Zr	B	C	Ni
LSHR	12.5	20.4	3.5	3.5	1.5	2.7	1.5	4.3	0.05	0.03	0.045	Bal
ME3	13	21	3.4	3.8	0.8	3.7	2.4	2.1	0.05	0.02	0.05	Bal



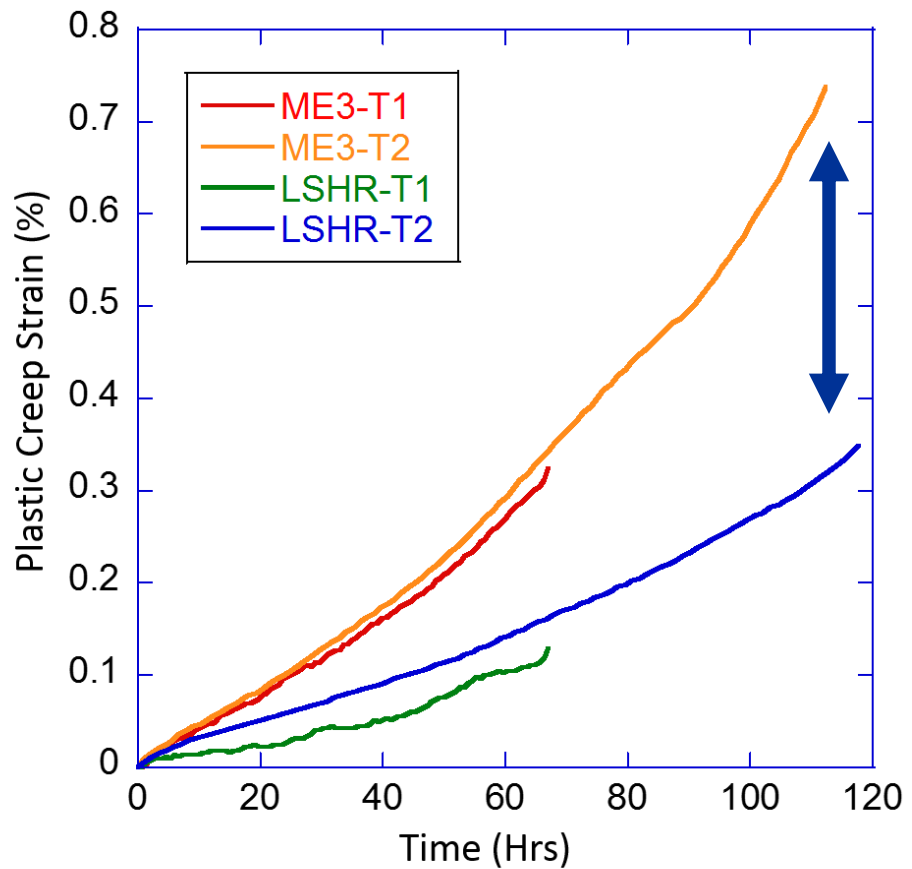
ME3 Average Grain Diameter = 59.2  $\mu\text{m}$   
 LSHR Average Grain Diameter = 59.9  $\mu\text{m}$



Alloy	Secondary $\gamma'$ VF	Tertiary $\gamma'$ VF	Total $\gamma'$ VF	Average Secondary $\gamma'$ Size	Average Tertiary $\gamma'$ Size
ME3	$43.97 \pm .6$	$2.65 \pm .4$	$46.61 \pm 1.0$	135 nm	15.4 nm
LSHR	$43.52 \pm 1.7$	$2.27 \pm .1$	$45.80 \pm 1.8$	154 nm	15.9 nm

The two alloys are  
microstructurally comparable!

# Creep Testing of ME3 and LSHR

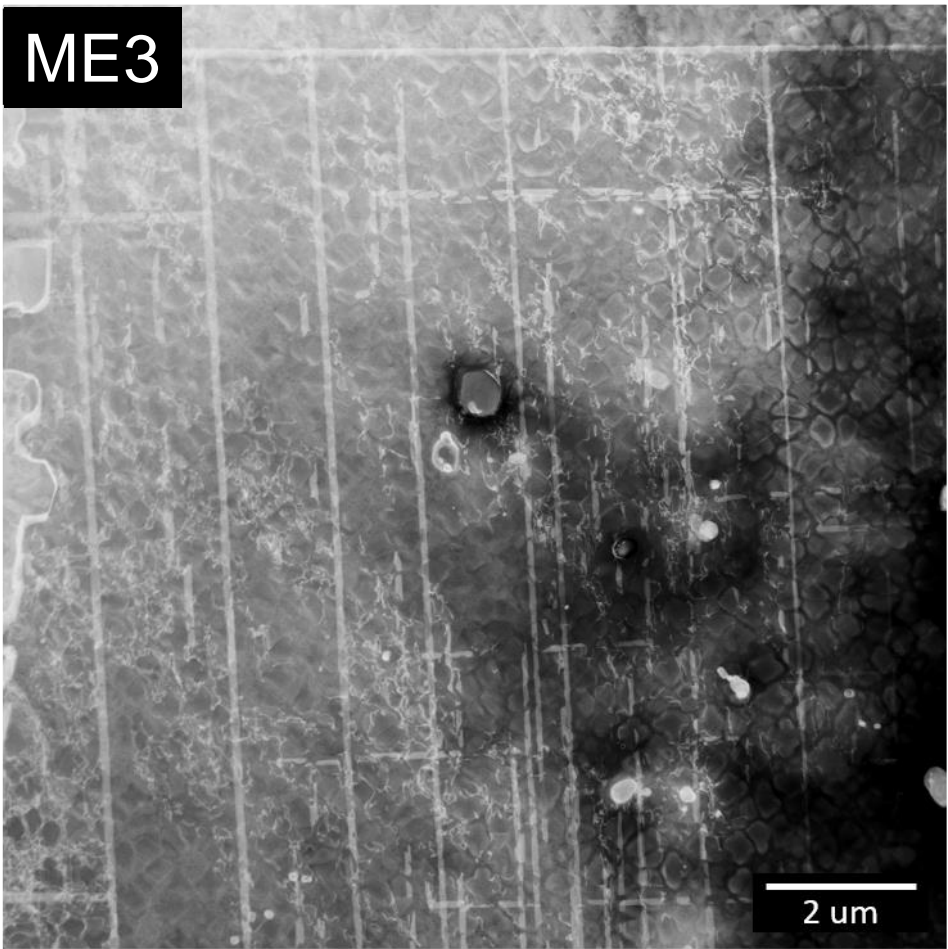


Creep tests were performed at 760°C under a stress of 552MPa

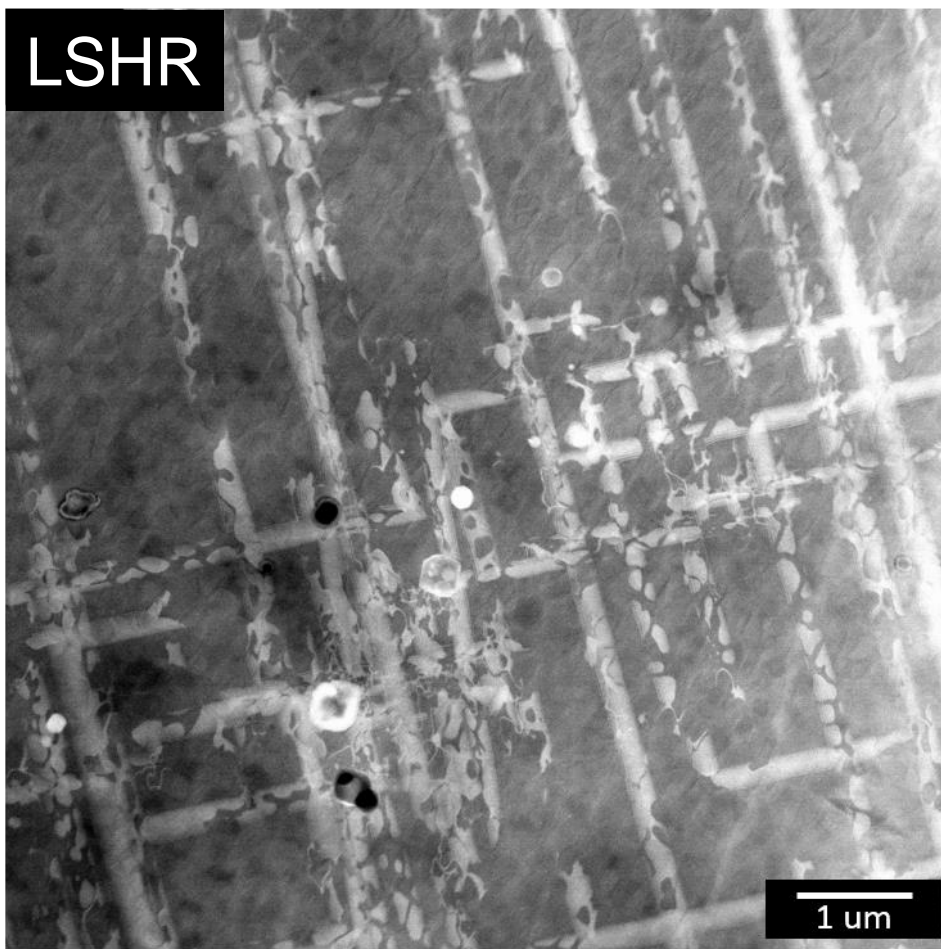
LSHR has consistently performed better in creep compared to ME3 in this temperature regime. Why?

# Scanning Transmission Electron Microscopy Characterization

ME3



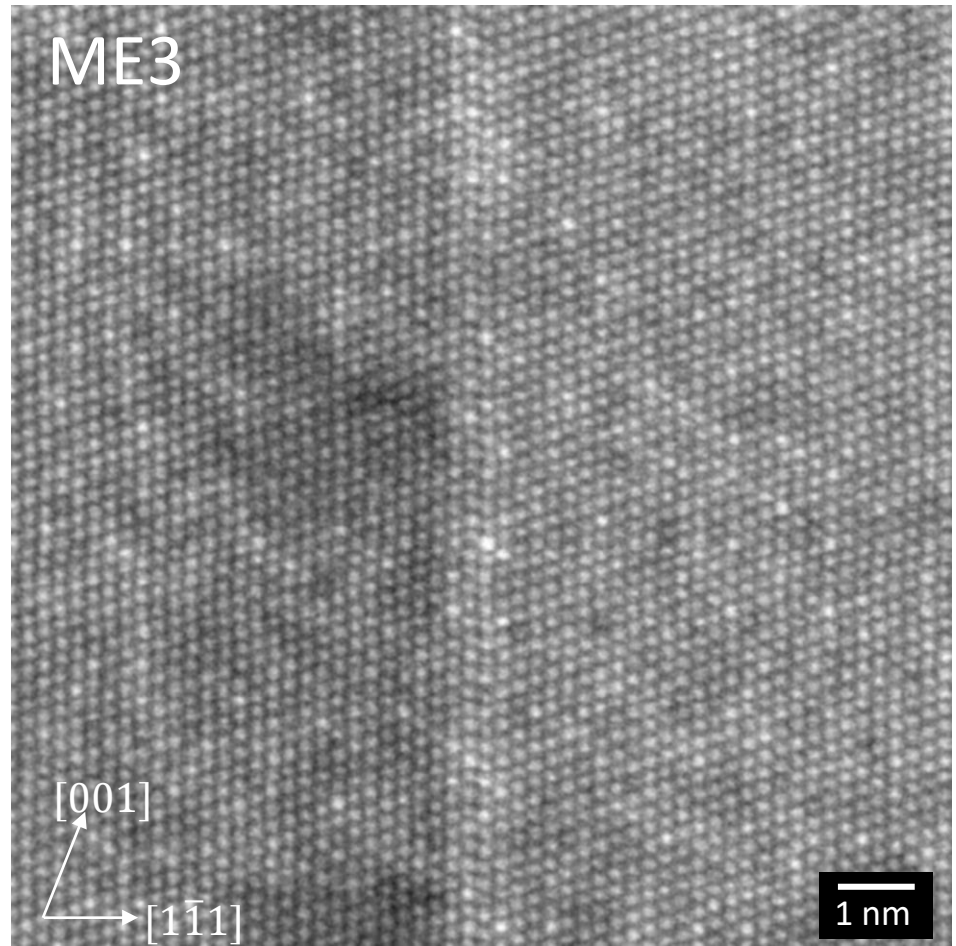
LSHR



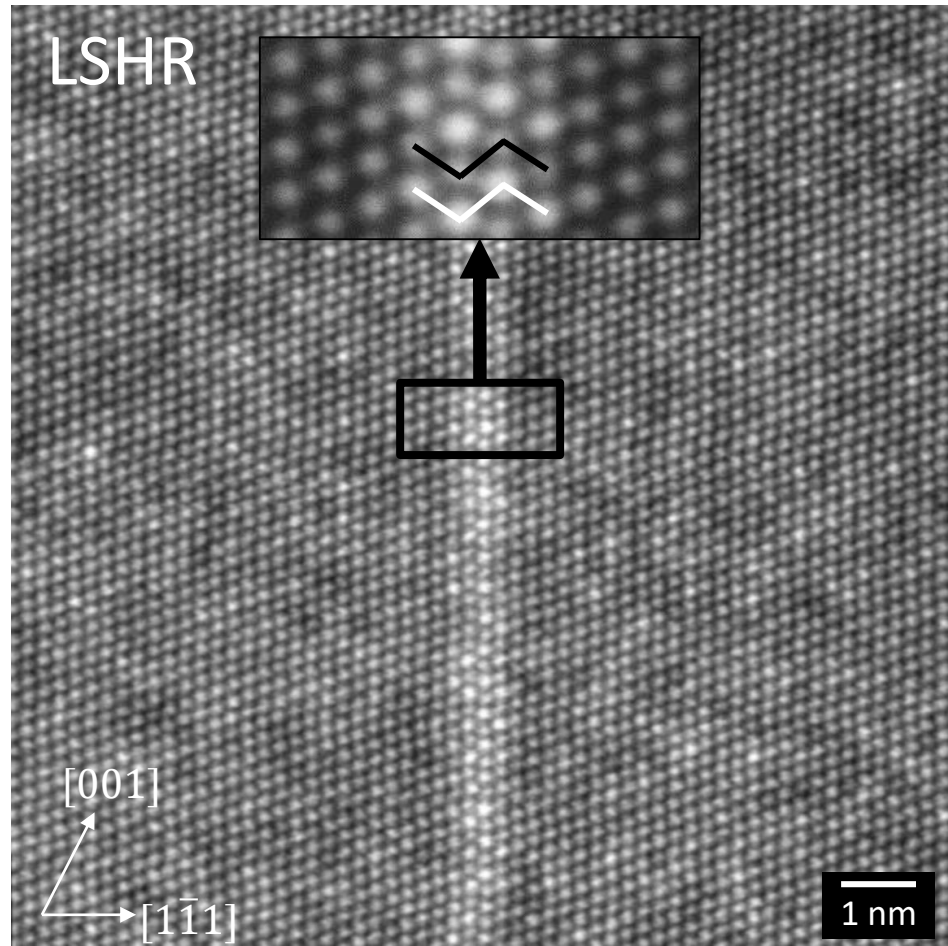
No notable differences in active deformation modes could be discerned between the two alloys.

# Segregation along SISFs in ME3 and LSHR

ME3

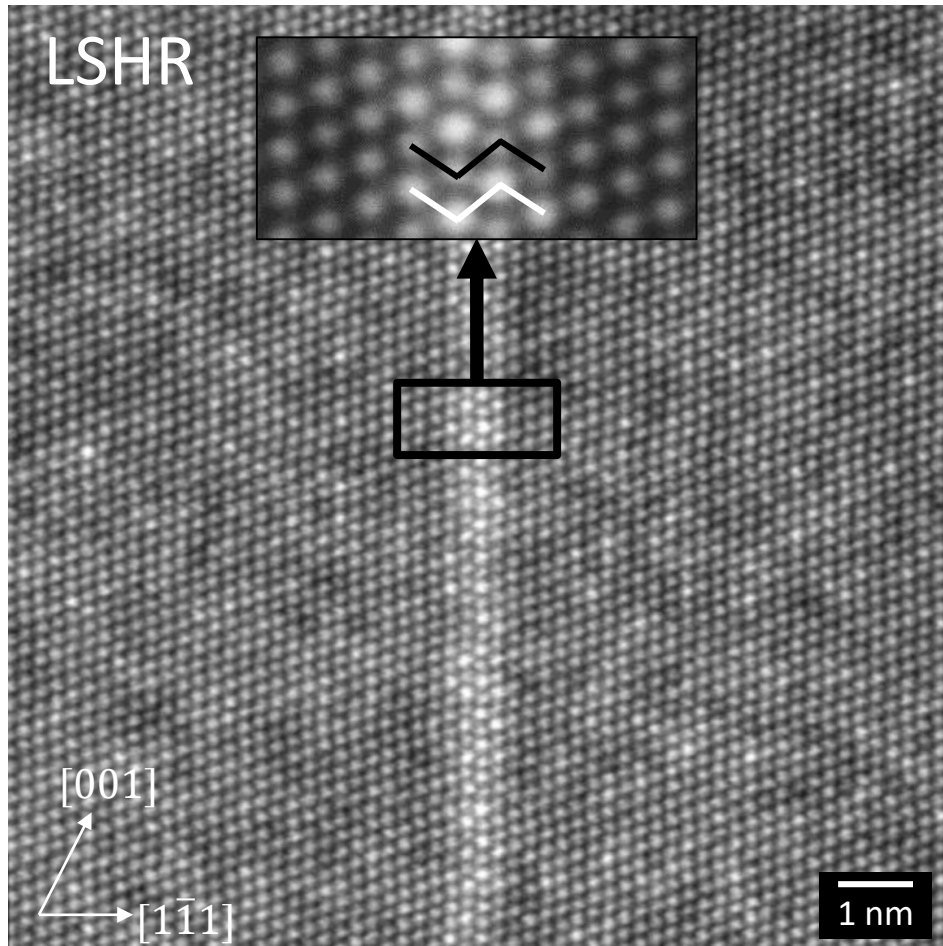
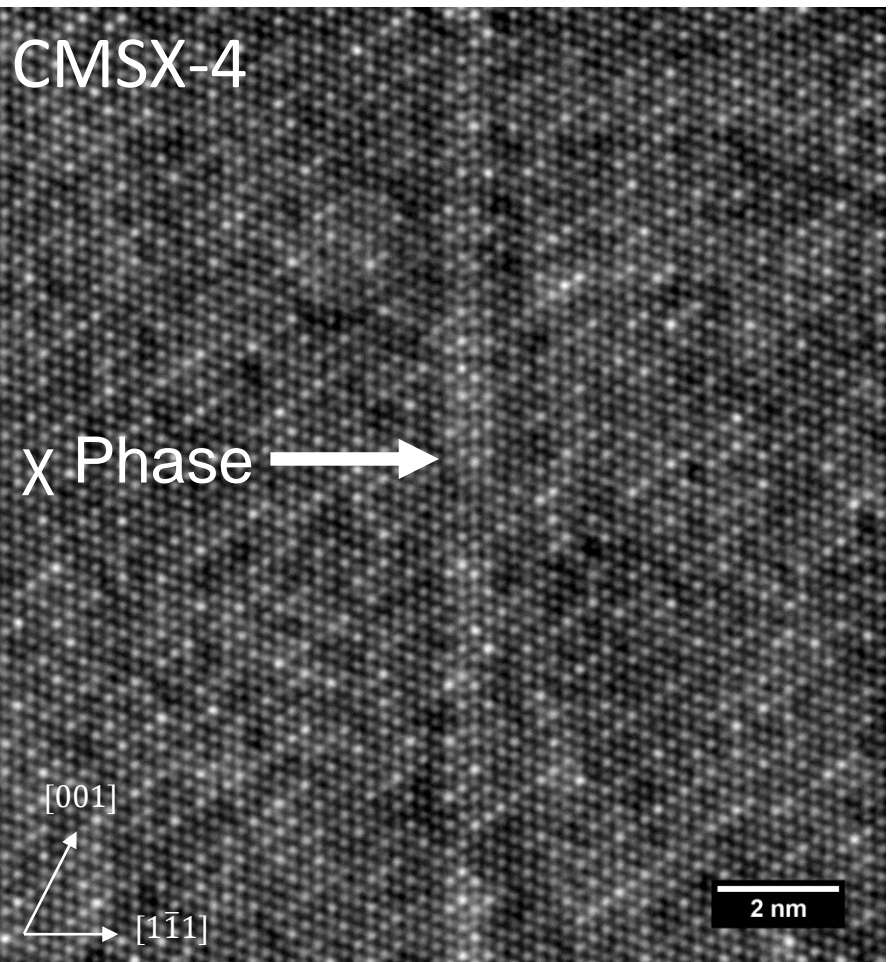


LSHR



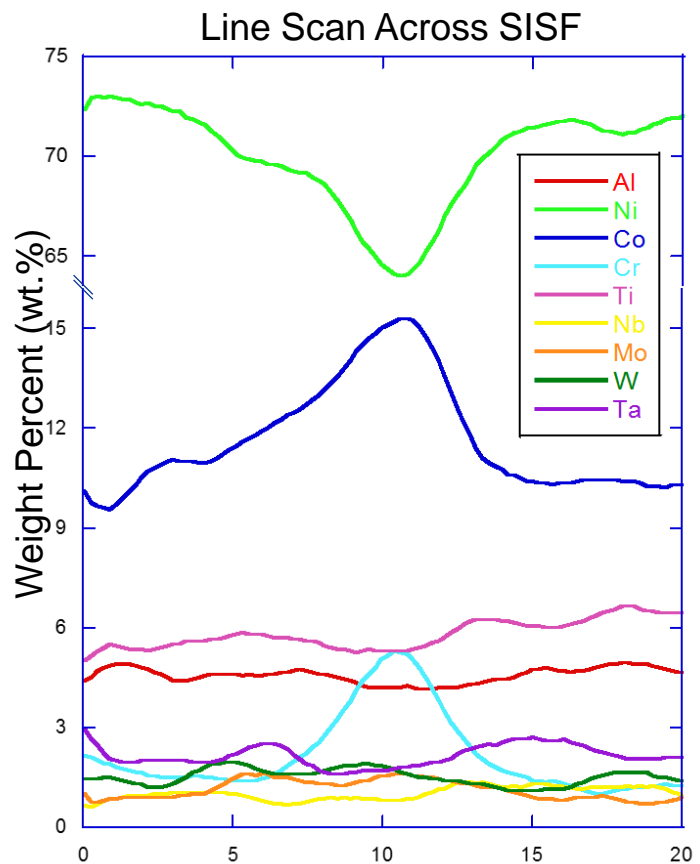
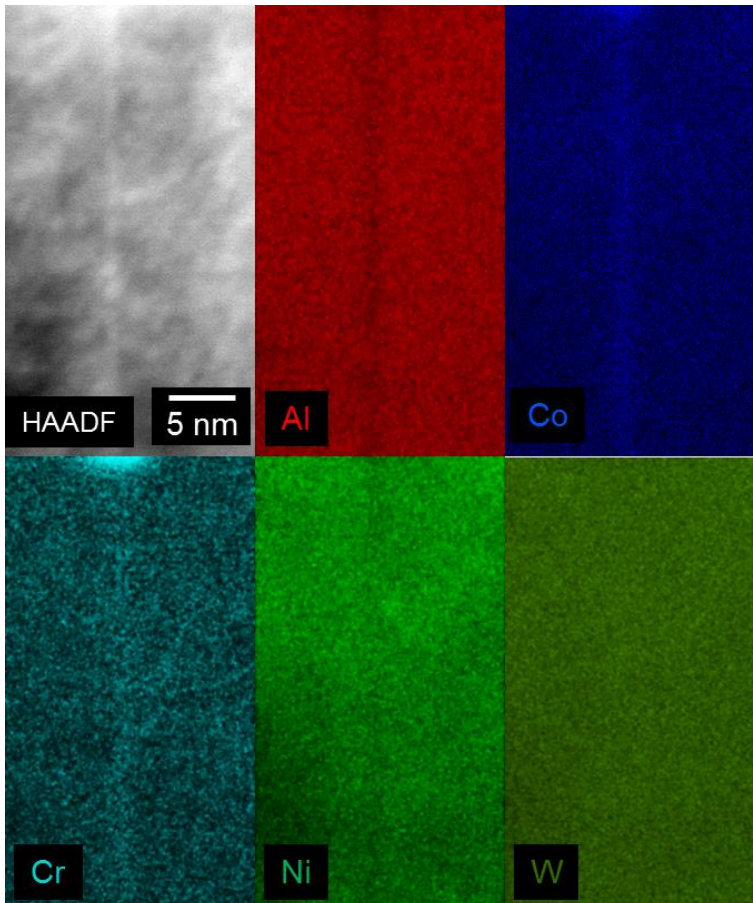
Ordered contrast exists along SISFs in LSHR but not ME3

# Segregation along SISFs in ME3 and LSHR



Ordered contrast exists along SISFs in LSHR but not ME3

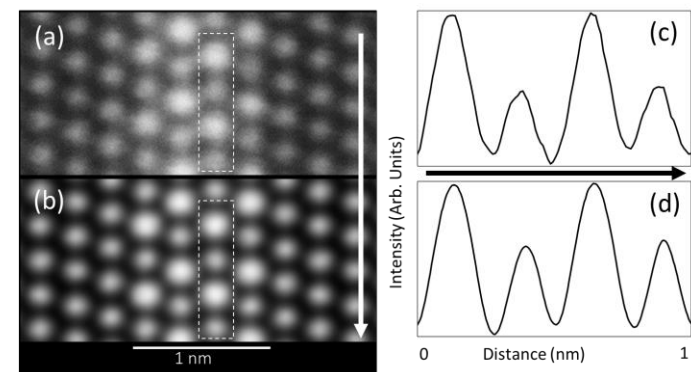
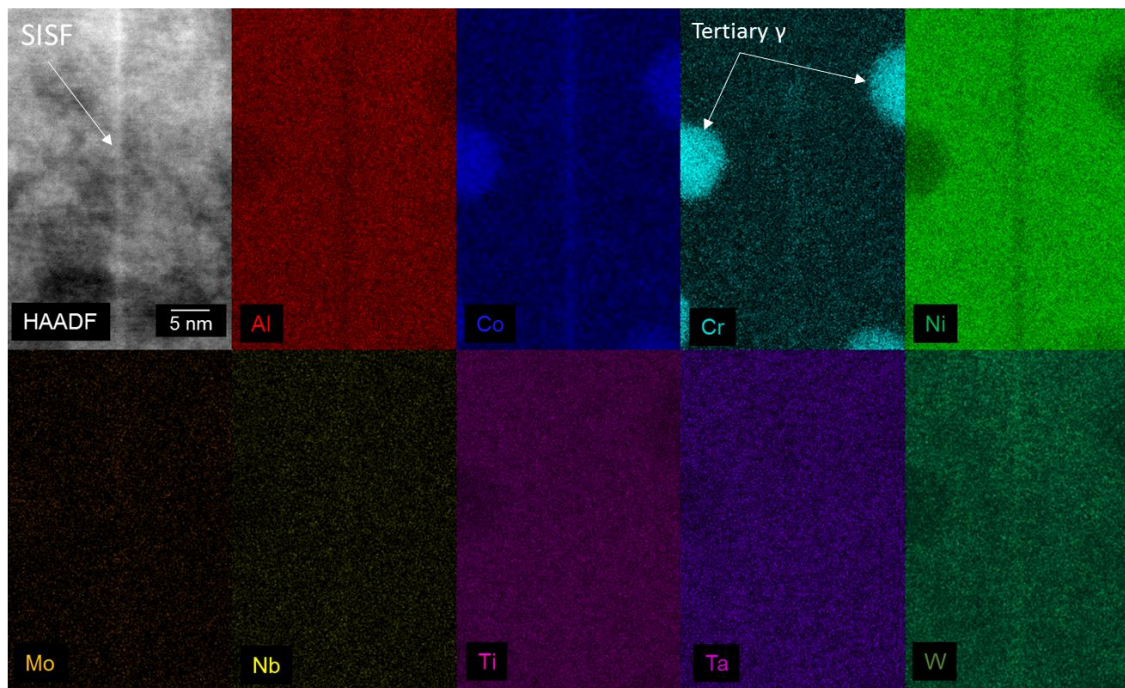
# Segregation along SISFs – ME3



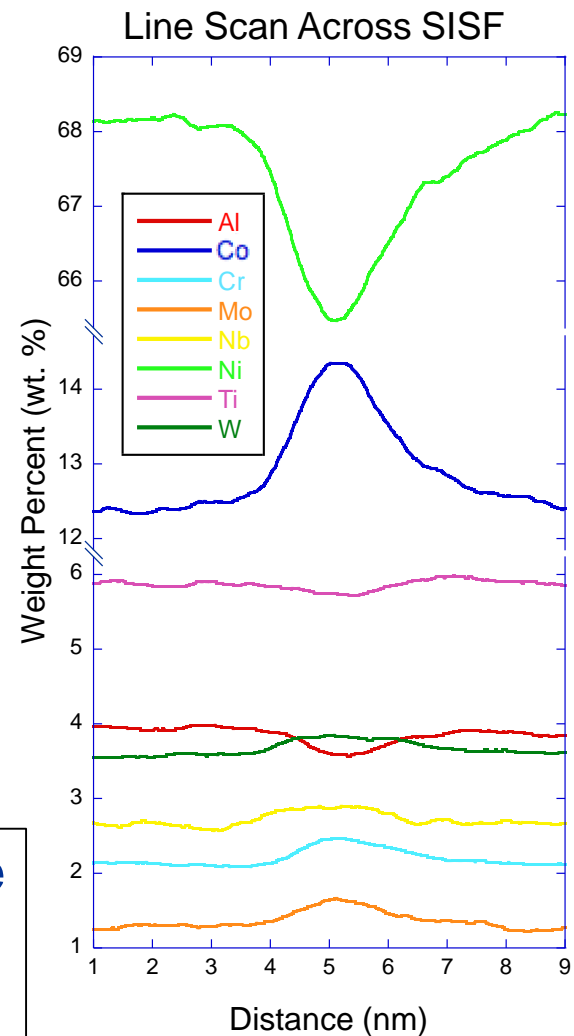
Confirmed  $\gamma$  phase nucleation  
along SISFs in ME3

Co, Cr Segregation  
Ni, Al Depletion

# Segregation along SISFs - LSHR

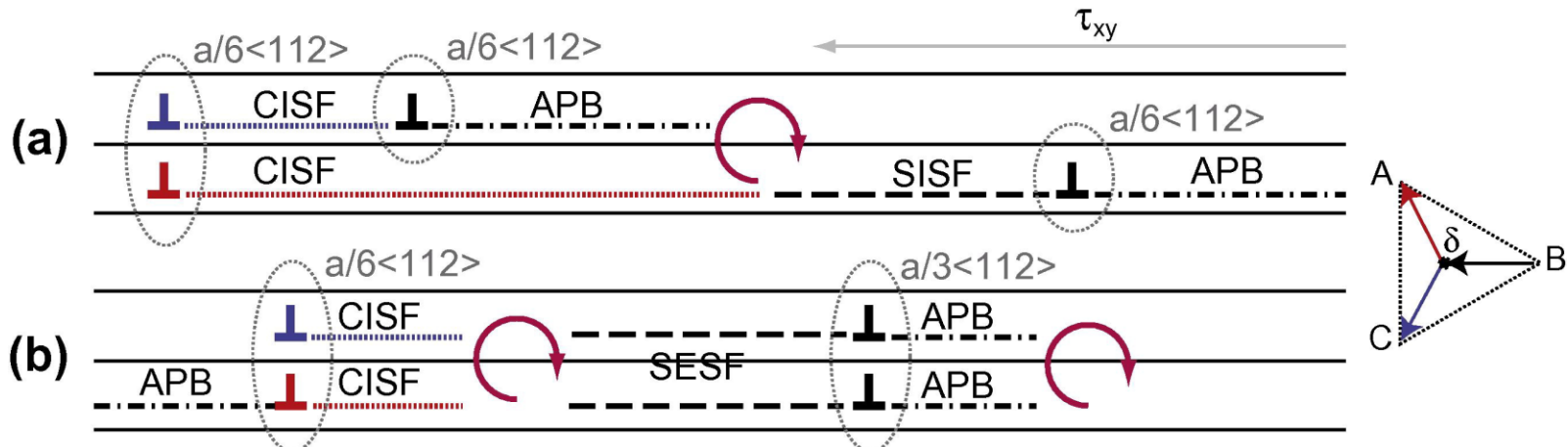


Confirmed x phase  
nucleation along  
SISFs in LSHR



Co, W, Cr Segregation  
Ni, Al Depletion

# Stacking Fault Ribbon Formation



Vorontsov et al. Acta Materialia. 2012

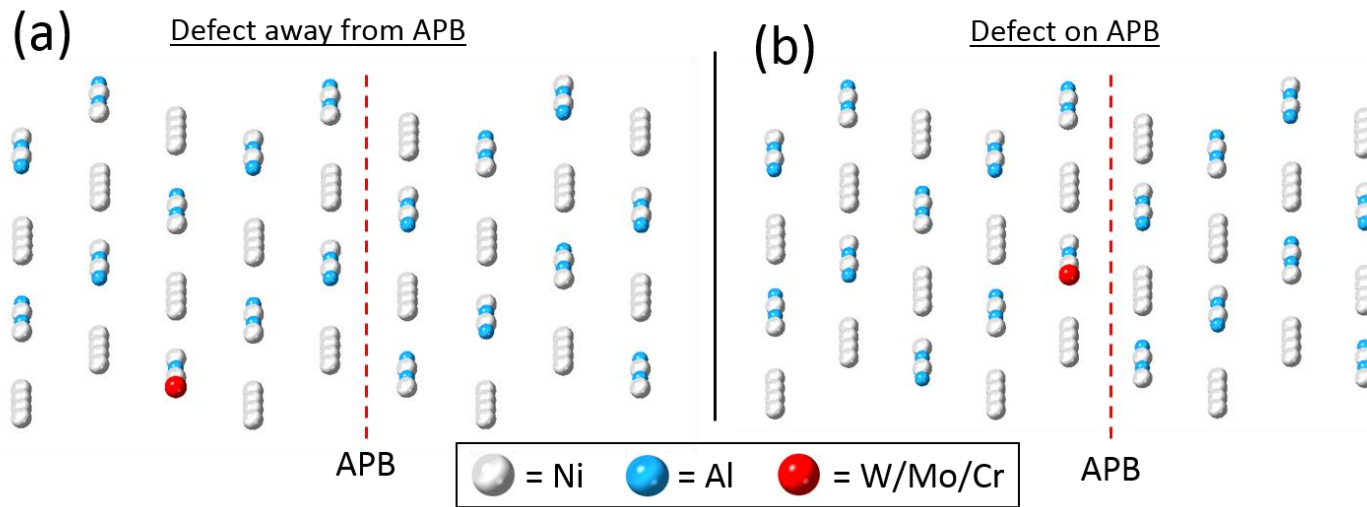
$$\frac{a}{3} < 112 > (\text{SISF}) + \frac{a}{6} < 112 > (\text{APB}) + \frac{a}{6} < 112 > (\text{SESF}) + \frac{a}{3} < 112 > = a < 112 >$$

Stacking Fault ribbons are a major source of primary creep strain in this temperature regime for single crystal superalloys

C.M.F. Rae and R.C. Reed. Acta Materialia. 2007

What effects will  $\gamma$  or  $\chi$  phase formation along SISFs have on this shearing process?

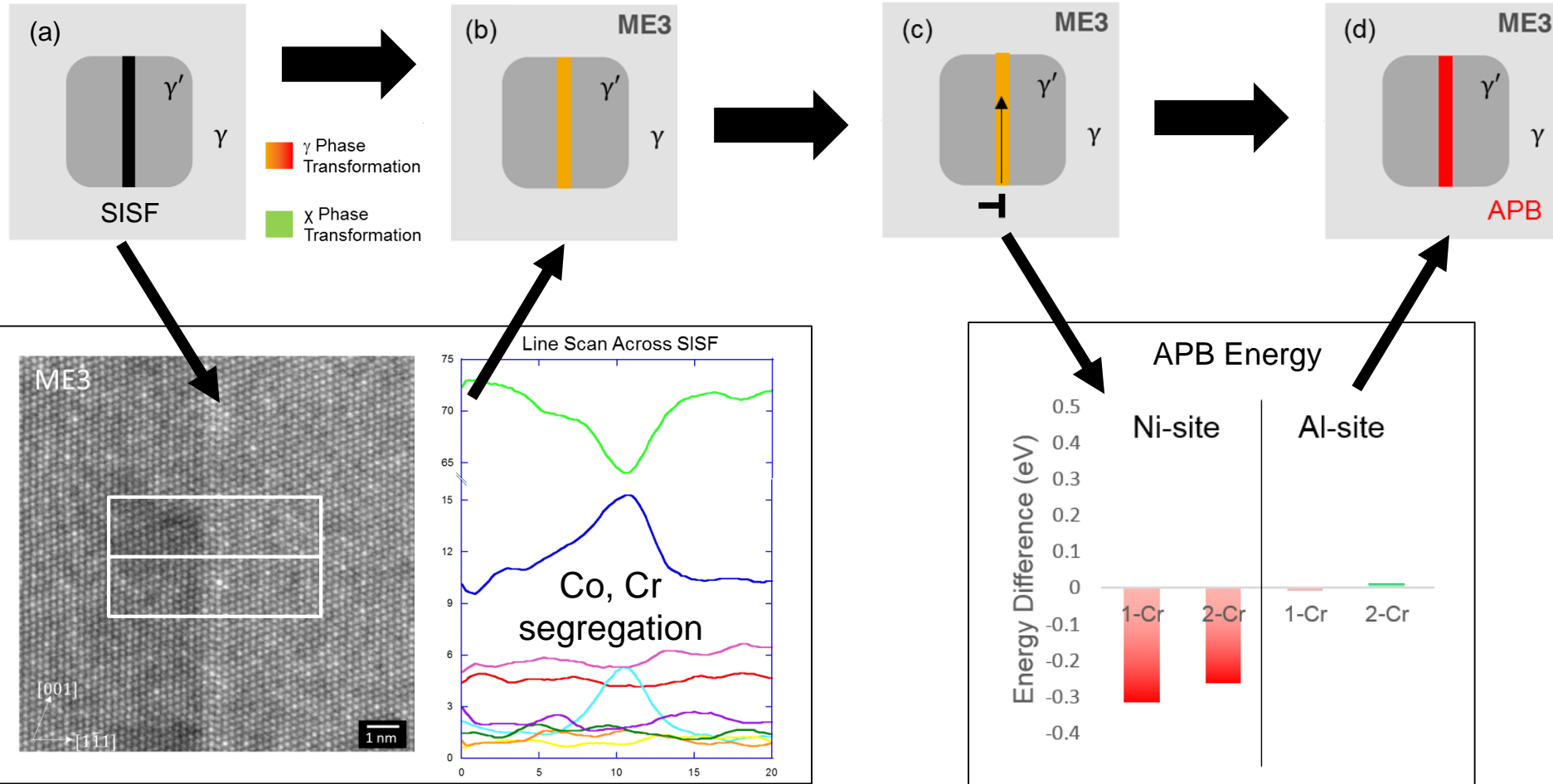
# Density Functional Theory Measurements



$\text{Ni}_3\text{Al}$   $\gamma'$  cells with an APB were created to explore the effect SISF segregation has on the formation of the trailing APB.

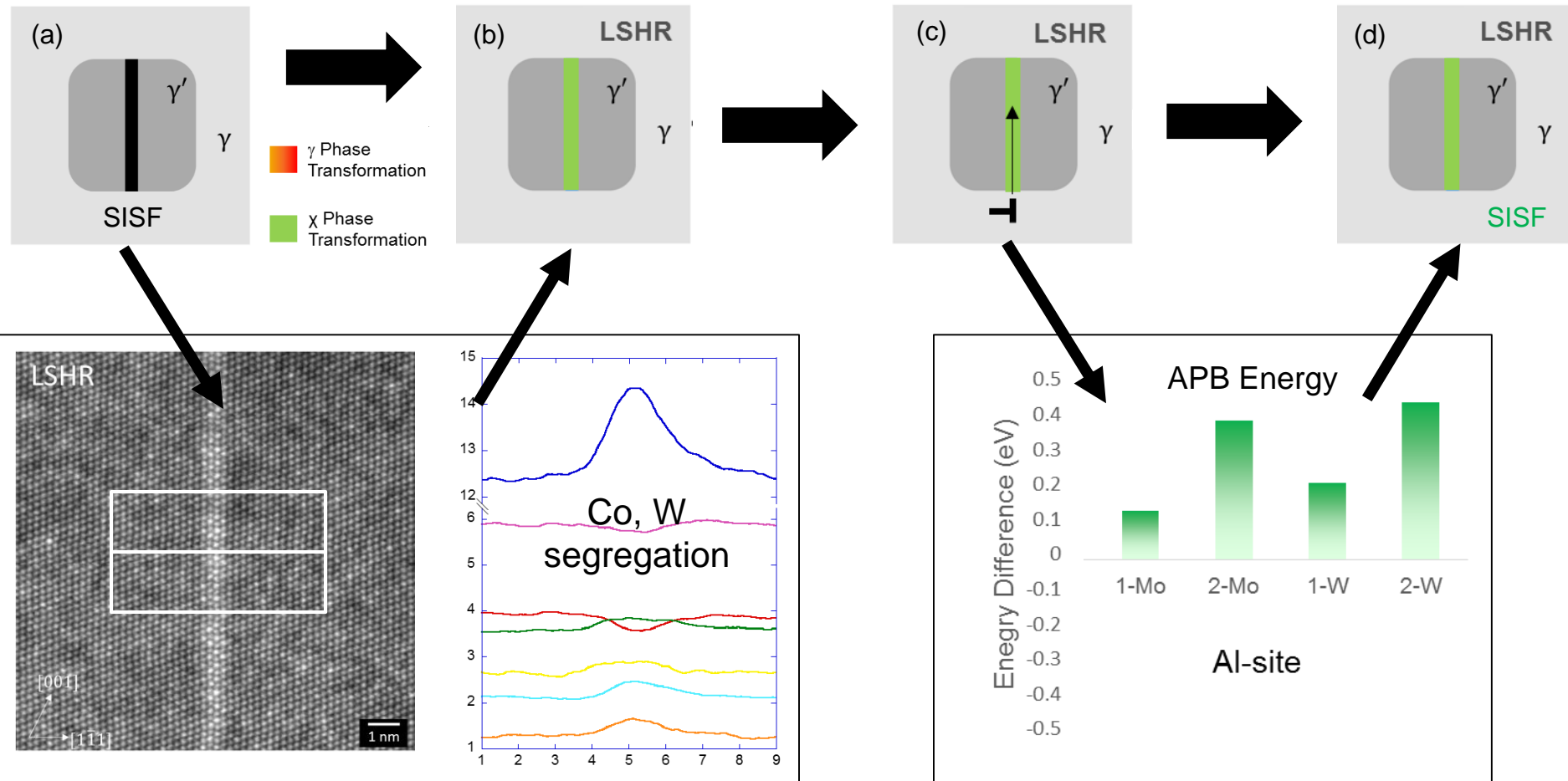
Relaxed energies were compared when a W, Mo, or Cr atom were away from the APB or on the APB.

# Phase Transformation Softening – $\gamma$ Phase



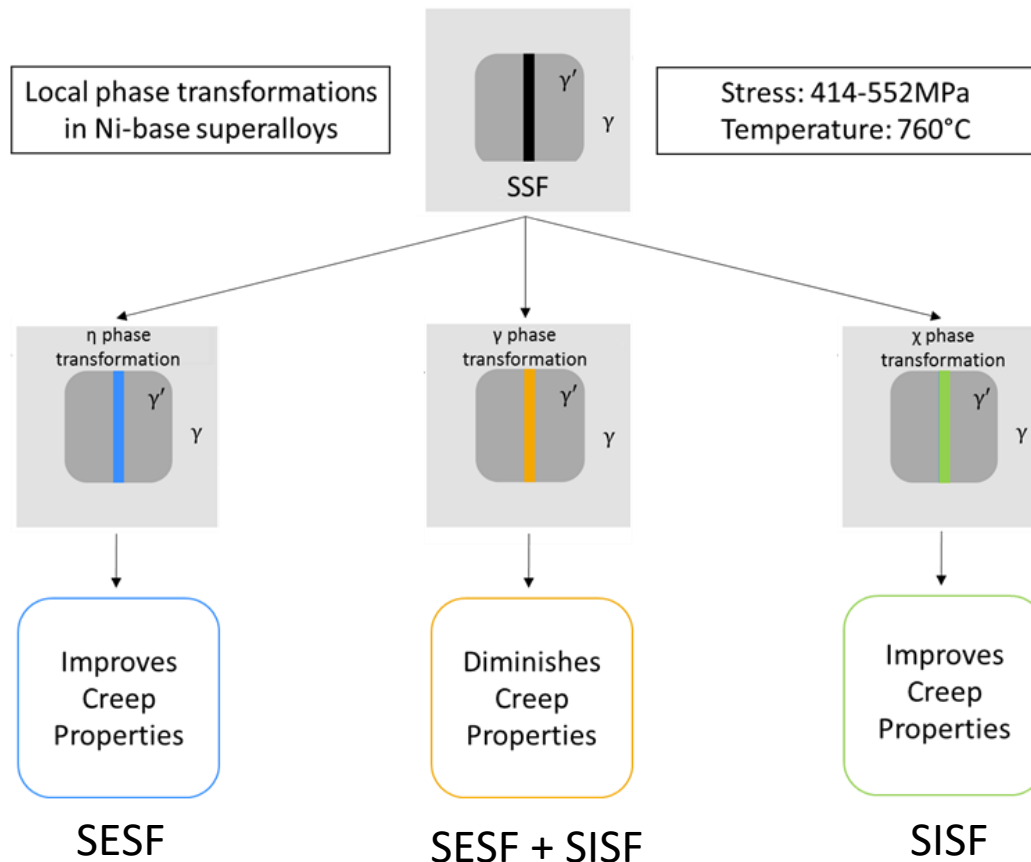
$\gamma$  phase formation along SISF promotes stacking fault ribbon shear

# Phase Transformation Strengthening – x phase



x phase formation along SISF inhibits stacking fault ribbon shear

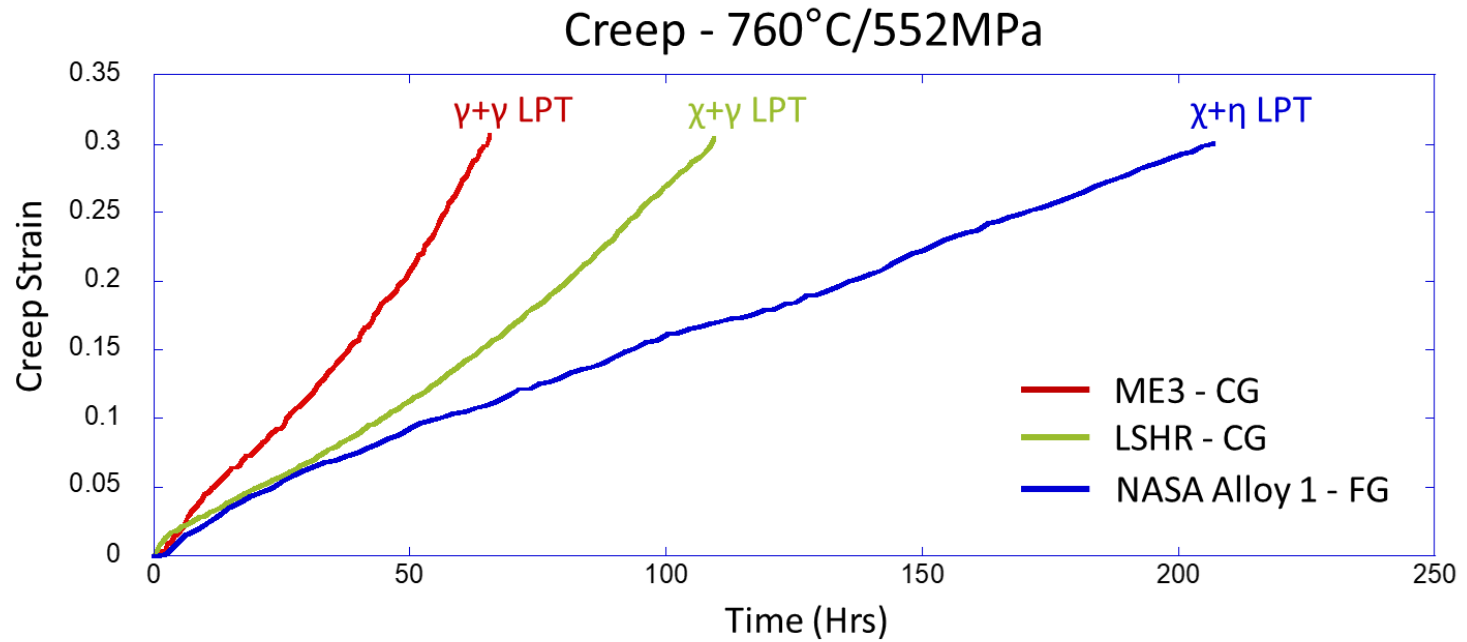
# Phase Transformation Strengthened Superalloys



Can the  $\eta$  and  $\chi$  phase transformation strengthening mechanisms be combined into a single alloy without precipitating bulk topologically close packed (TCP) phases?



# NASA Alloy 1



**Conclusion:** NASA Alloy 1 presents significantly better creep properties over current state of the art alloys through phase transformation strengthening



# Part 2: Efficient Production of a High Performance Dispersion Strengthened, Multi-principal element alloy

TM Smith<sup>1</sup>, AC Thompson<sup>2</sup>, TP Gabb<sup>1</sup>, RB Rogers<sup>1</sup>, MJ Kulis<sup>1</sup>, KM Tacina<sup>1</sup>

<sup>1</sup>NASA Glenn Research Center, Cleveland Oh 44135 USA

<sup>2</sup>Vantage Partners, 3000 Aerospace Pkwy, Brook Park, OH 44142, USA

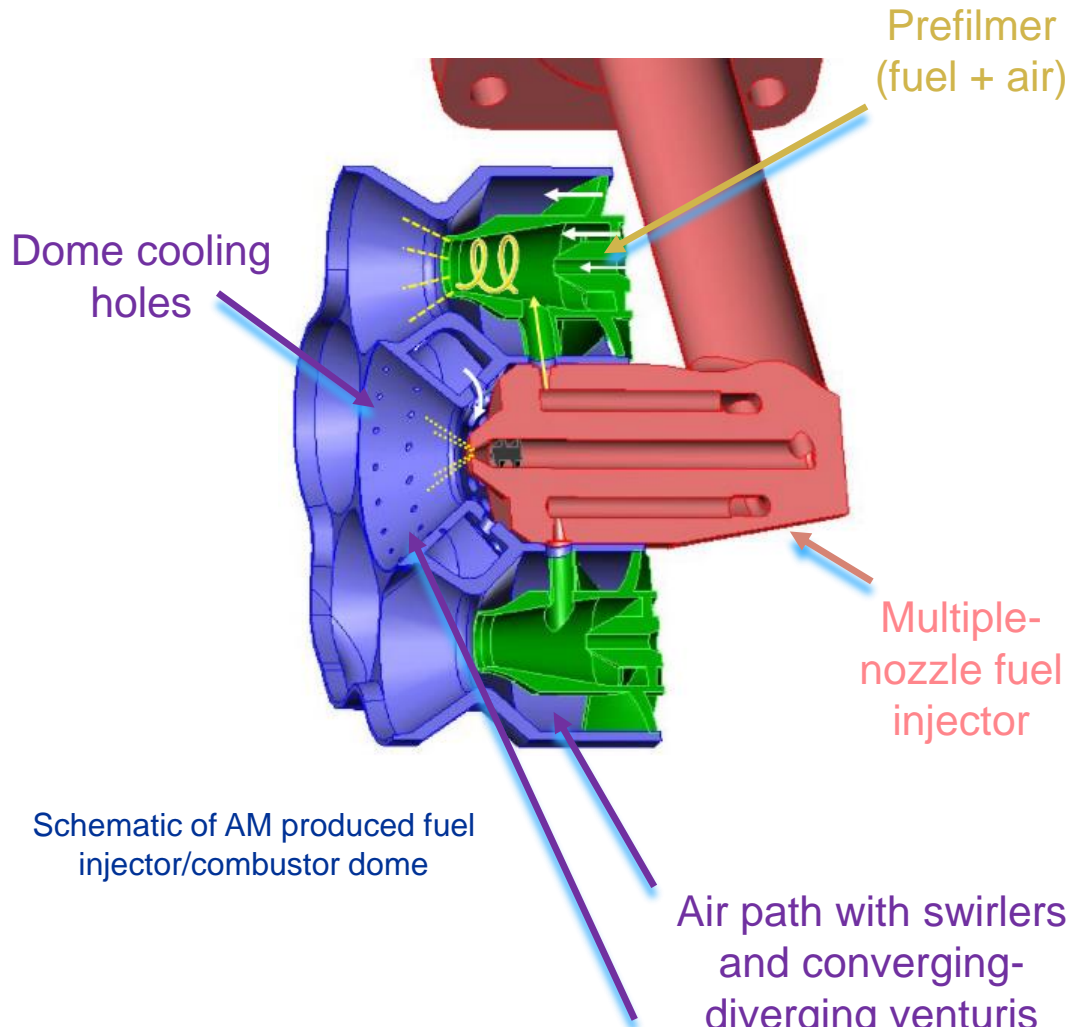
*Support provided by NASA's Aeronautics Research Mission Directorate (ARMD) Transformational Tools and Technologies (TTT) Project Office*

# Background – NASA Application

**Problem:** Conventional materials and processing techniques limit the design of combustor domes used in jet turbine engines.

**Proposed Solution:** Develop a high ductility, high temperature material for an additively-manufactured (AM) combustor fuel nozzle and dome for supersonic aircraft ( $>1093^{\circ}\text{C}$  ( $2000^{\circ}\text{F}$ ) operating temperature).

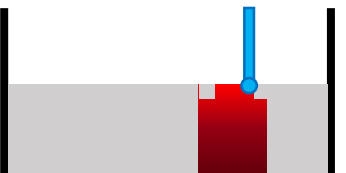
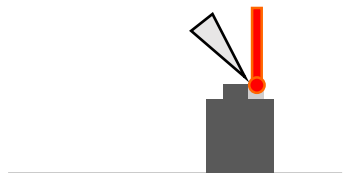
- Lead to several improvements to the turbine combustor design ultimately reducing NOx pollution and lowering weight.
- May enable lean-front-end small-core combustors.



Schematic of AM produced fuel injector/combustor dome

Air path with swirlers and converging-diverging venturis

# Metallic Additive Manufacturing

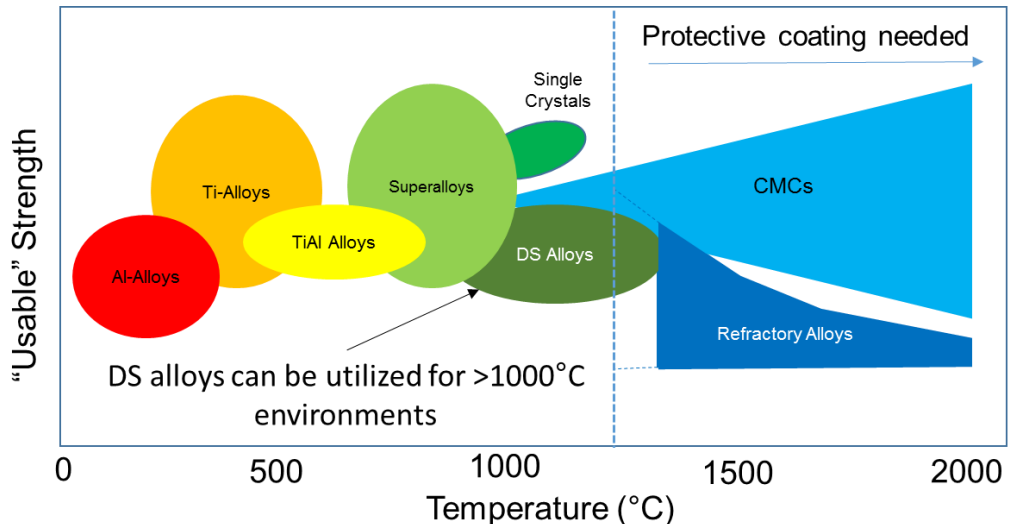
Process	Selective Laser Melting (SLM)	Electron Beam Melting (EBM)	Direct Energy Deposition (DED)
			
Energy Source	Laser	E-Beam	Laser or E-Beam
Powder Bed	Yes	Yes	No
Power (W or kV)	50-1000 W	<b>30-60kV</b>	100-2000 W
Max Build Size (mm)	500 x 280 x 320	500 x 280 x 320	<b>2000 x 1500 x 750</b>
Material	Metallic Powder	Metallic Powder	Metallic Powder or Wire
Dimensional Accuracy	<b>&lt;0.04 mm</b>	0.04-0.2 mm	0.5 mm (powder) 1.0 mm (wire)

- 3D printing or additive manufacturing (AM) has shown promise in realizing a new design space for aerospace applications.
- Each AM technique has a set of pros and cons associated with them.
- Instead of producing well known cast and wrought alloys with AM. We should look at AM as a new opportunity to produce materials that are currently difficult to create.
- For this study, SLM is used due to it's superior dimensional accuracy.

# High Temperature AM Compatible Materials

## High Temperature Materials:

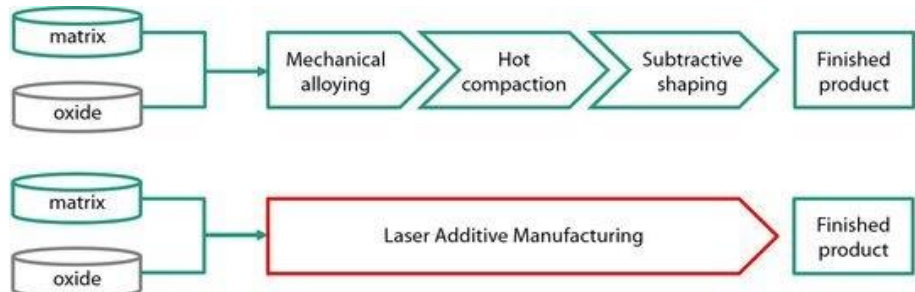
- Refractory metals
- Carbon-Carbon composites
- CMC's
- Ni-base superalloys
- **Dispersion strengthened (DS) alloys**



Inspired by Andy Jones. ODS alloy Development.

(DS) alloys offer higher temperature capabilities compared to Ni-base superalloys. However, it has been a challenge to produce DS alloys through conventional manufacturing methods.

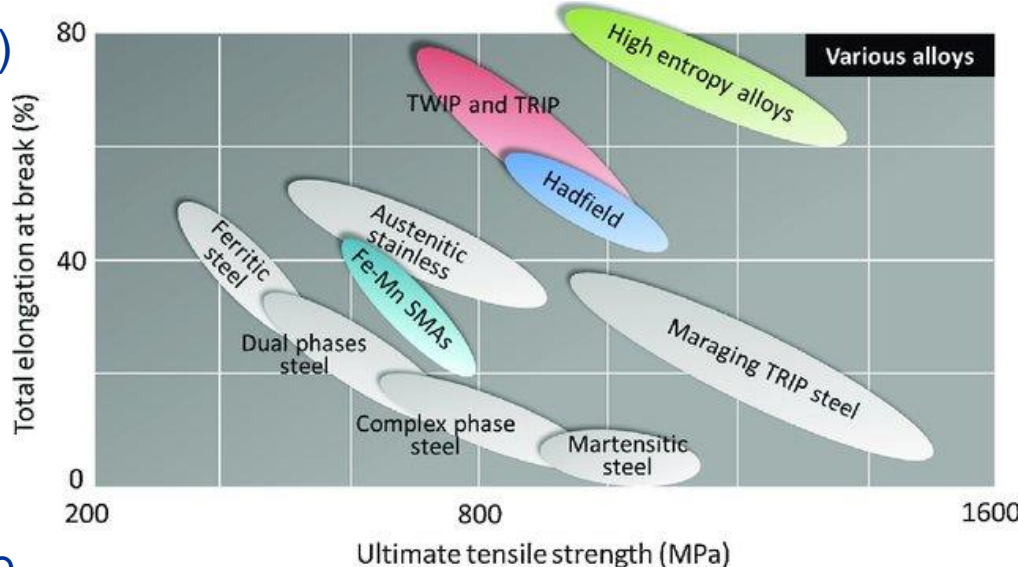
## Conventional Manufacturing vs AM



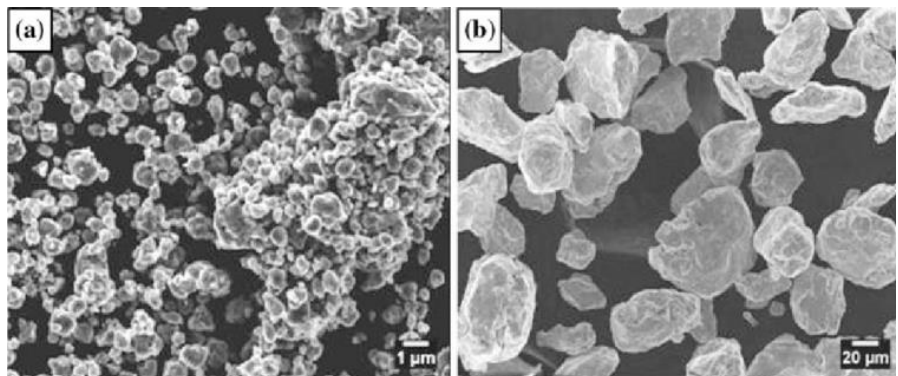
Can AM improve DS alloy manufacturability?

# Advanced Materials and Manufacturing for High Temperature Applications

- Multi-principal element alloys (MPEAs) or “High-entropy alloys” overcome the strength - ductility trade off.
- The equiautomic NiCoCr medium-entropy alloy (MEA) is particularly of interest due to it’s strong phase stability and mechanical properties.
- Single phase solid solution MPEAs are promising AM materials due to minor differences between their liquidus and solidus temperatures. This limits dendritic segregation, solidification cracking, and residual stress.
- **Can strengthening oxide particles be incorporated into the AM build without mechanical alloying?**



Chowdury *et al.* Materials Science and Engineering: Reports (2017)



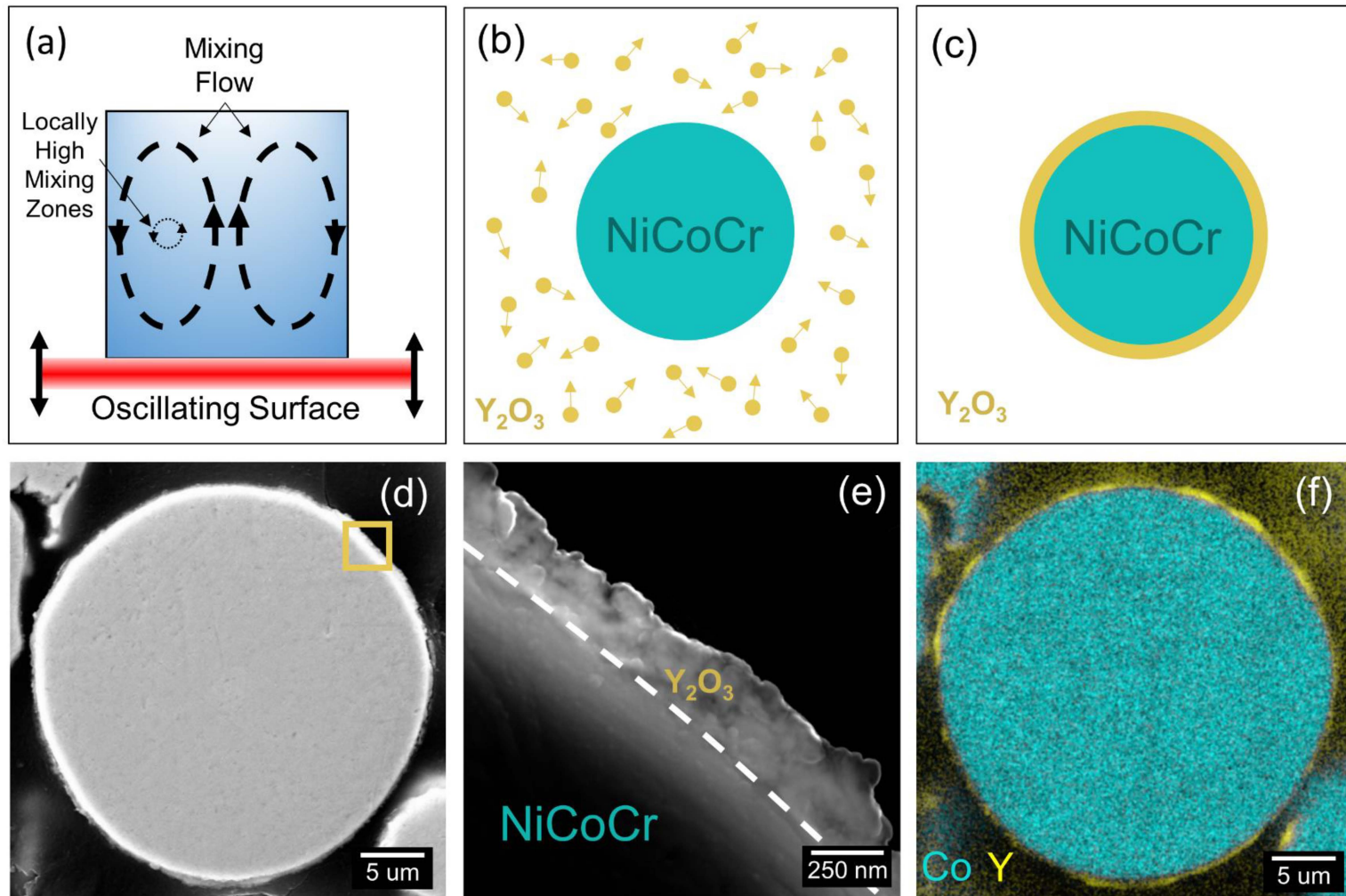
Oksiuta *et al.* Journal of Material Science (2010)



# Methods

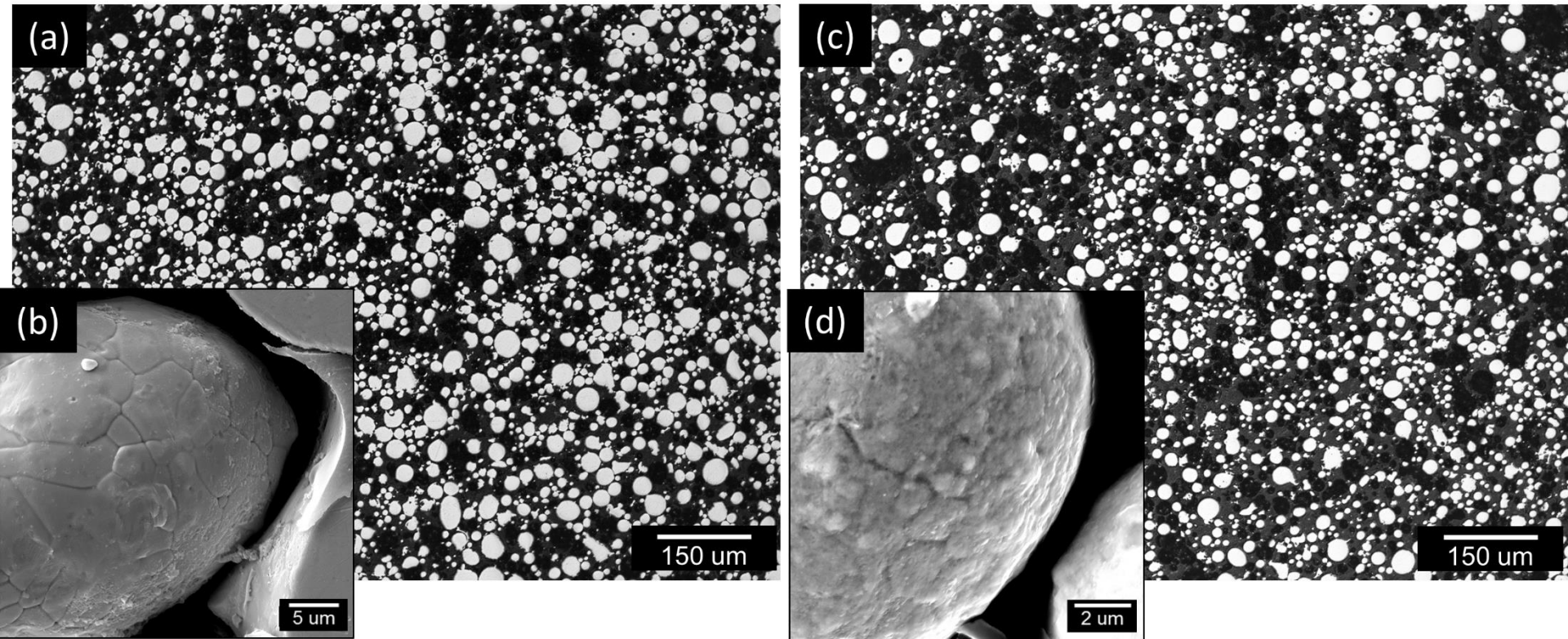
- Micron-scale (10-45um) NiCoCr powder was acquired from Praxair.
- Nano-scale (100-200nm) Yttria powder was acquired from American Elements.
- SLM Machine: EOS M100
- Powder Mixing: Resodyn LabRAM II
- Aim of study
  - Leverage SLM to produce dispersion strengthened multi-principal element alloys.
  - Determine optimal SLM laser parameters for both baseline (V-MEA) and dispersion strengthened (DS-MEA) builds.
  - Produce 99.9% dense vertical test specimen for microstructural and mechanical analysis using both V-MEA DS-MEA NiCoCr.
  - Explore heat treatment effects on mechanical performance
  - Produce a high temperature capable 3D printed combustor dome.

# Novel Powder Coating Technique



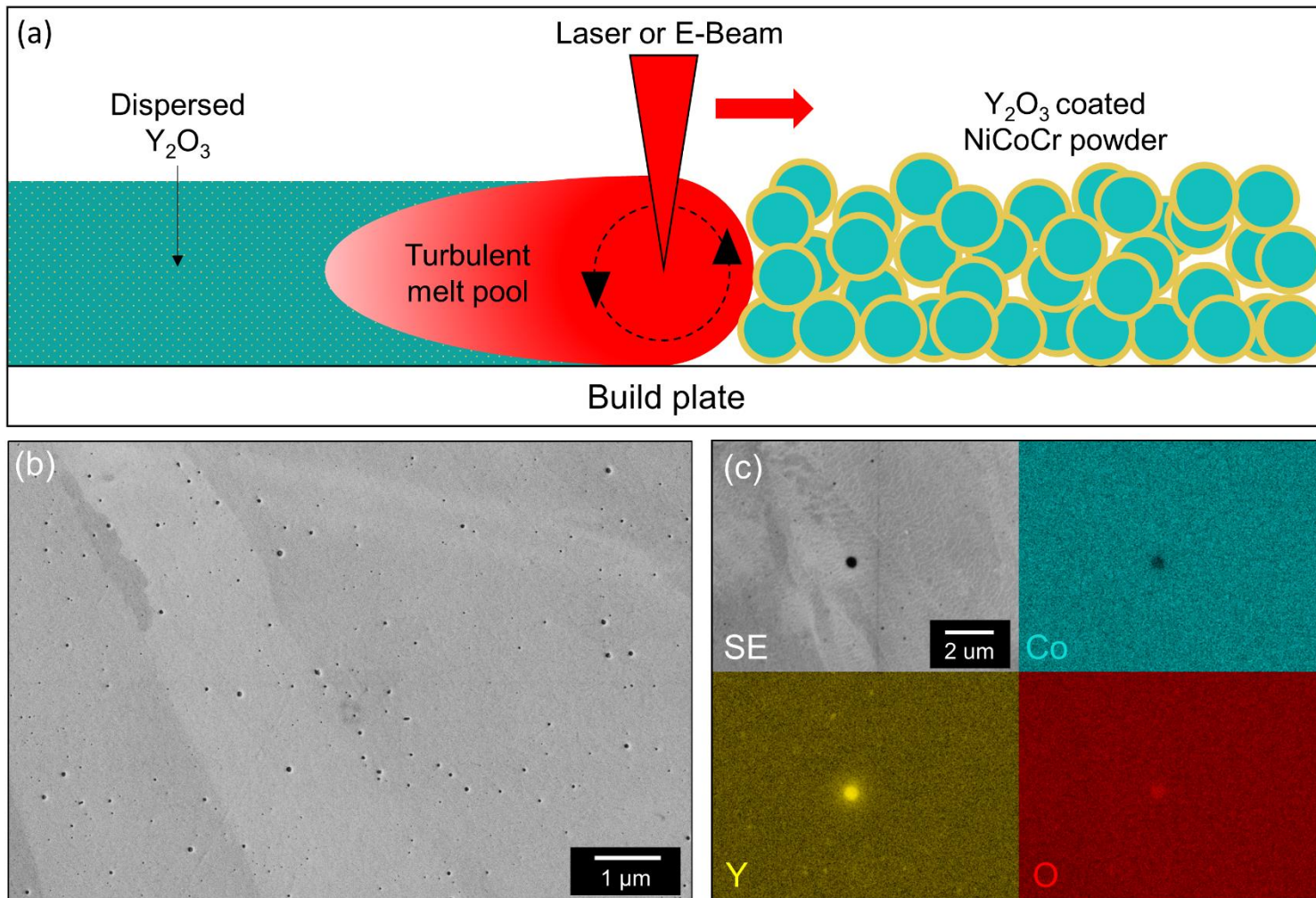
New high energy mixing technique successfully coats NiCoCr powder with 1 wt.% Yttria.

# Novel Powder Coating Technique



- The resonant mixing technique did not deform the NiCoCr powders.
- Both uncoated and coated powders qualitatively passed the Hall flow test.

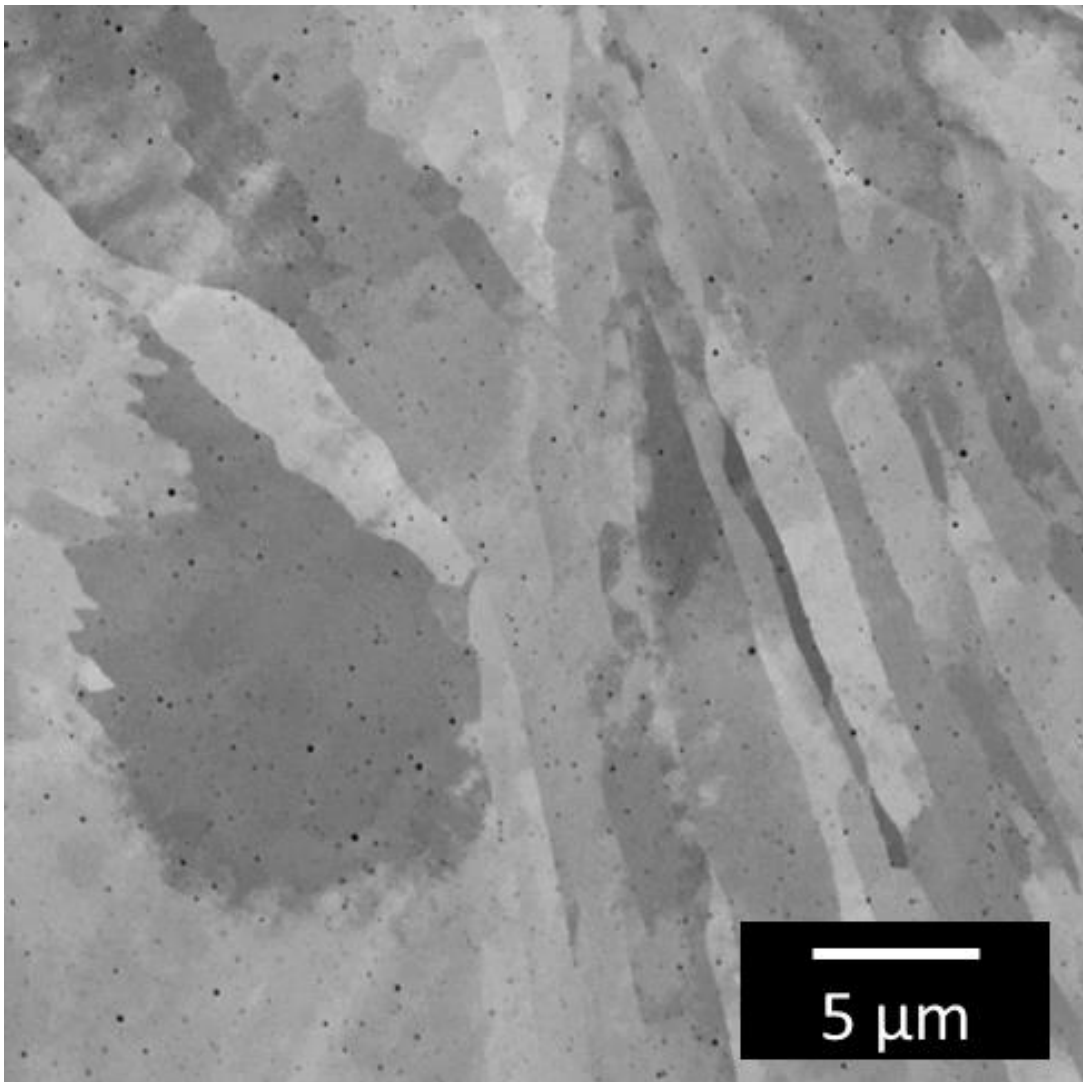
# Leveraging SLM to Produce Dispersion Strengthened Alloys



SLM successfully disperses the nano-scale Yttria particles throughout the AM build

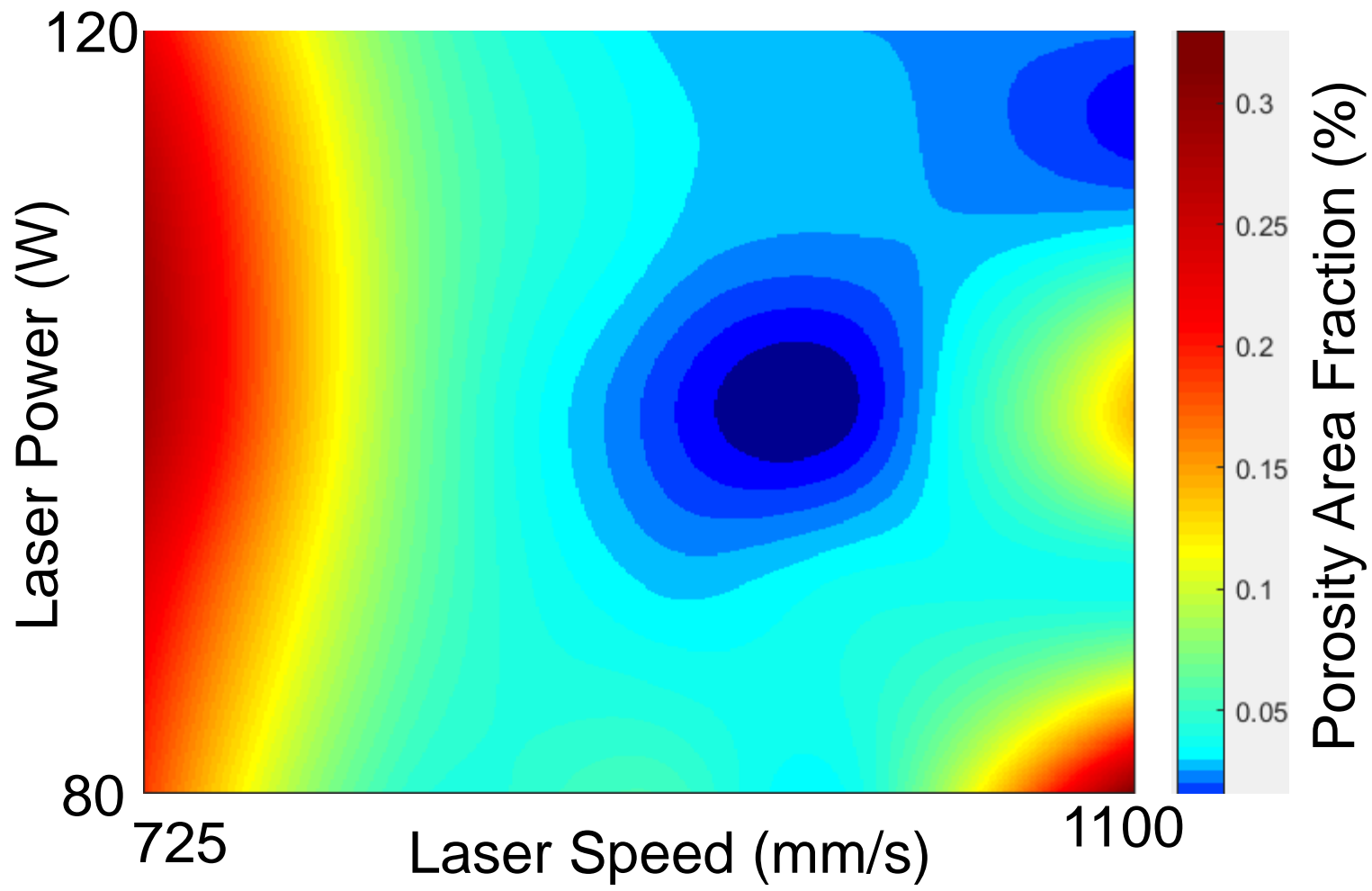


# DS-MEA Microstructure



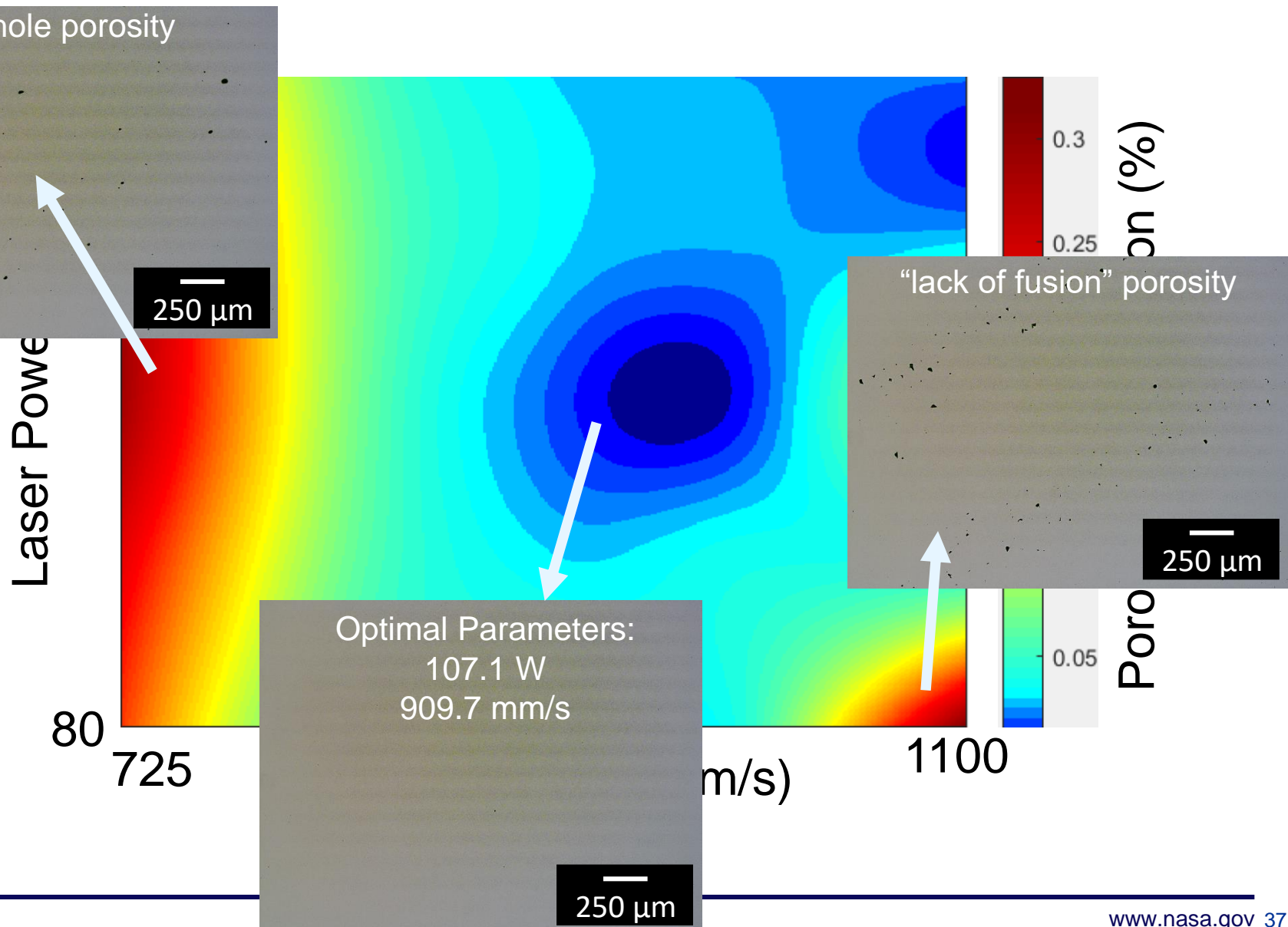
Nano-scale  $\text{Y}_2\text{O}_3$  particles are randomly dispersed throughout microstructure.

# SLM Laser Parameters V-MEA



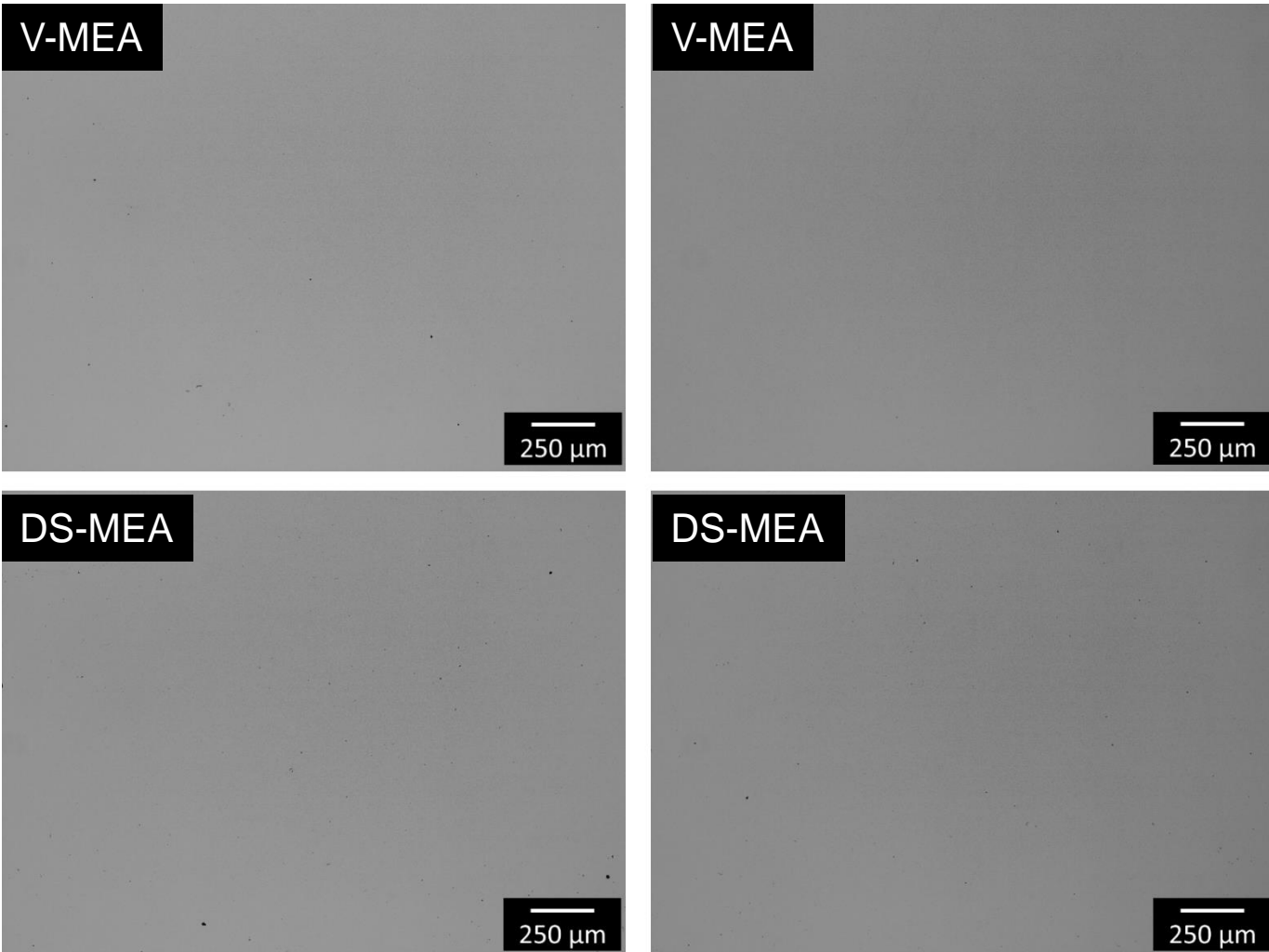
# SLM Laser Parameters V-MEA

Keyhole porosity



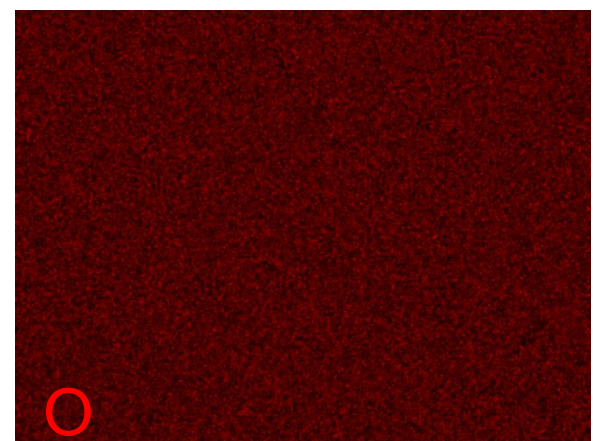
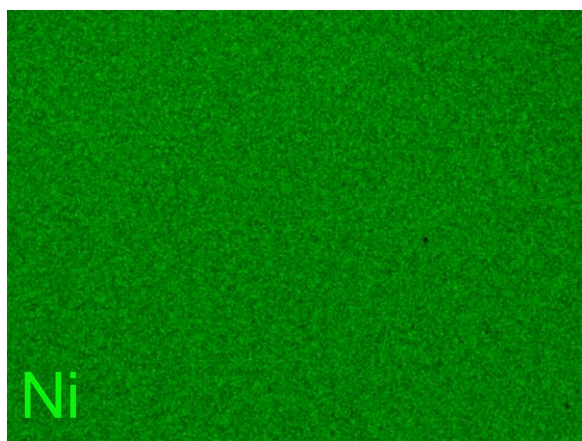
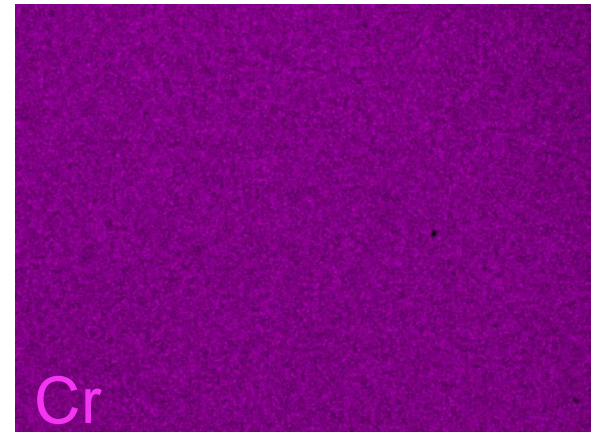
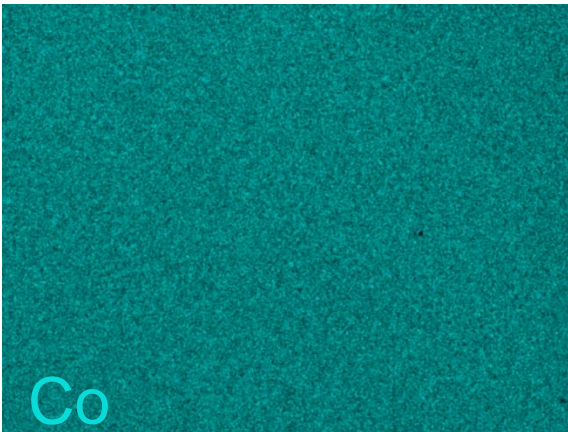
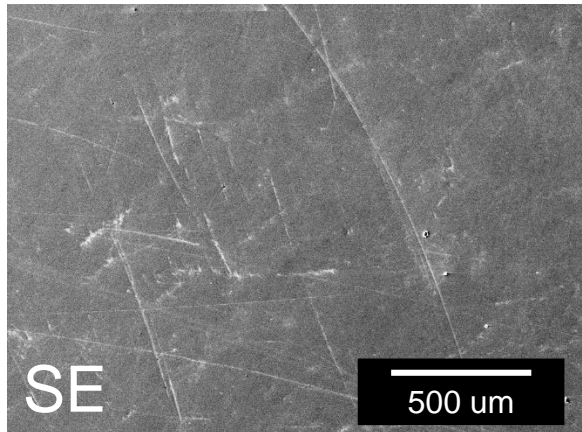


# MEA Microstructures - Porosity



99.9% dense parts were successfully built for both the V-MEA and DS-MEA powder lots.

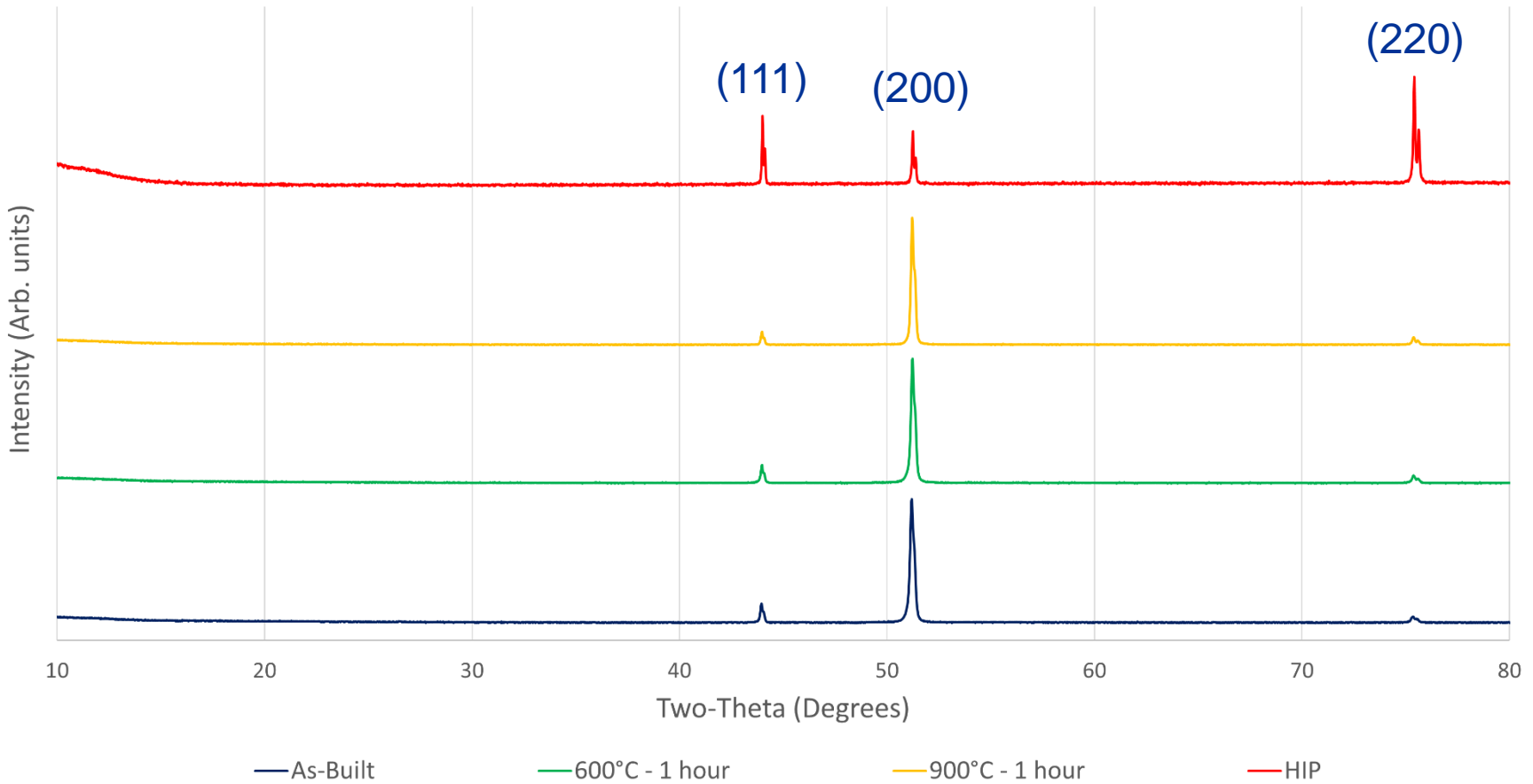
# EDS – DS-MEA Microstructure



- Large (>20um)  $\text{Y}_2\text{O}_3$  particles are not present in AM builds
- NiCoCr matrix remained a random solid solution during SLM process.

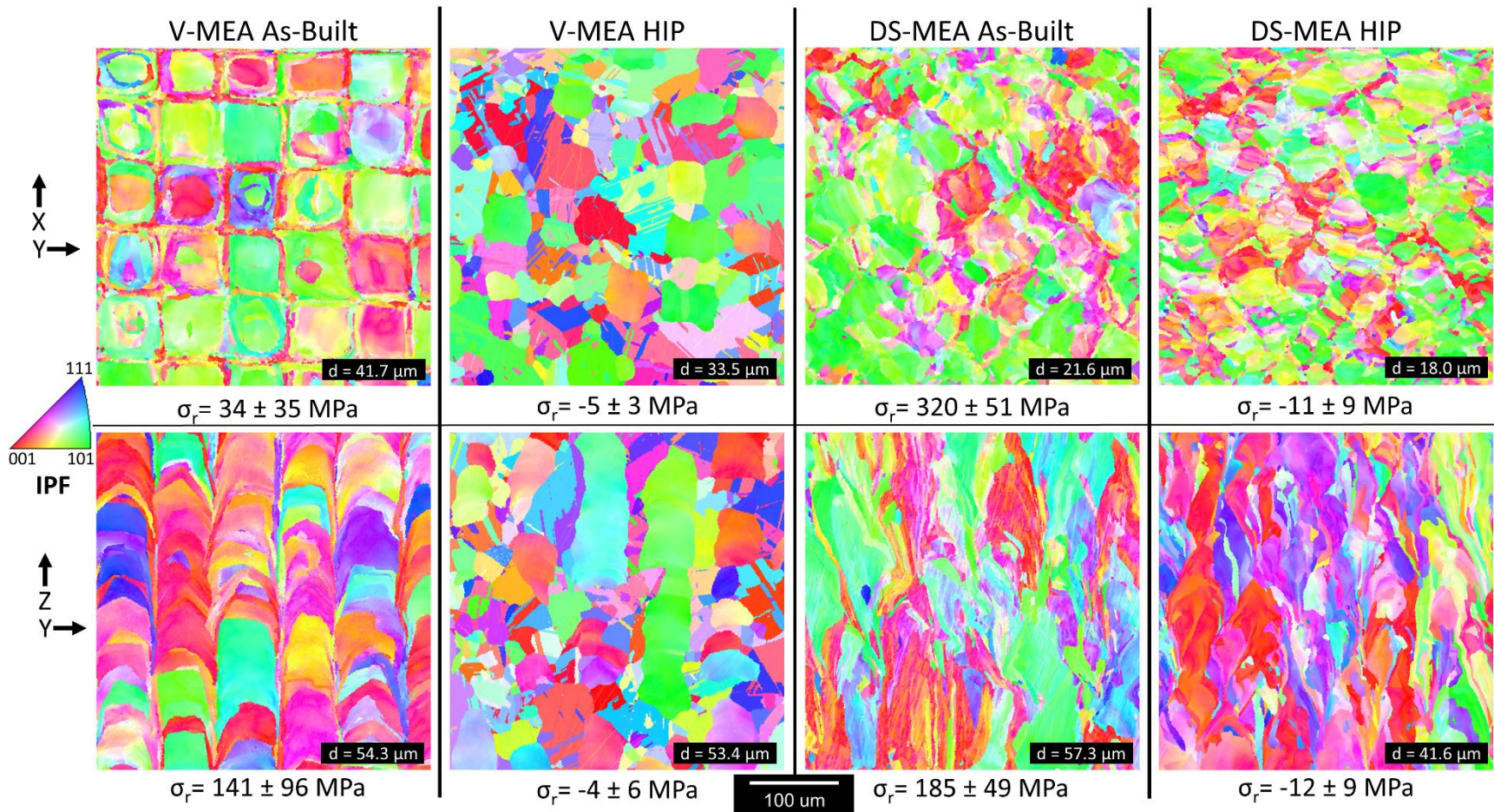
# Heat Treatment effect on solid solution stability

X-Ray Diffraction - V-MEA



No intermetallic phases present after anneal or HIP steps.

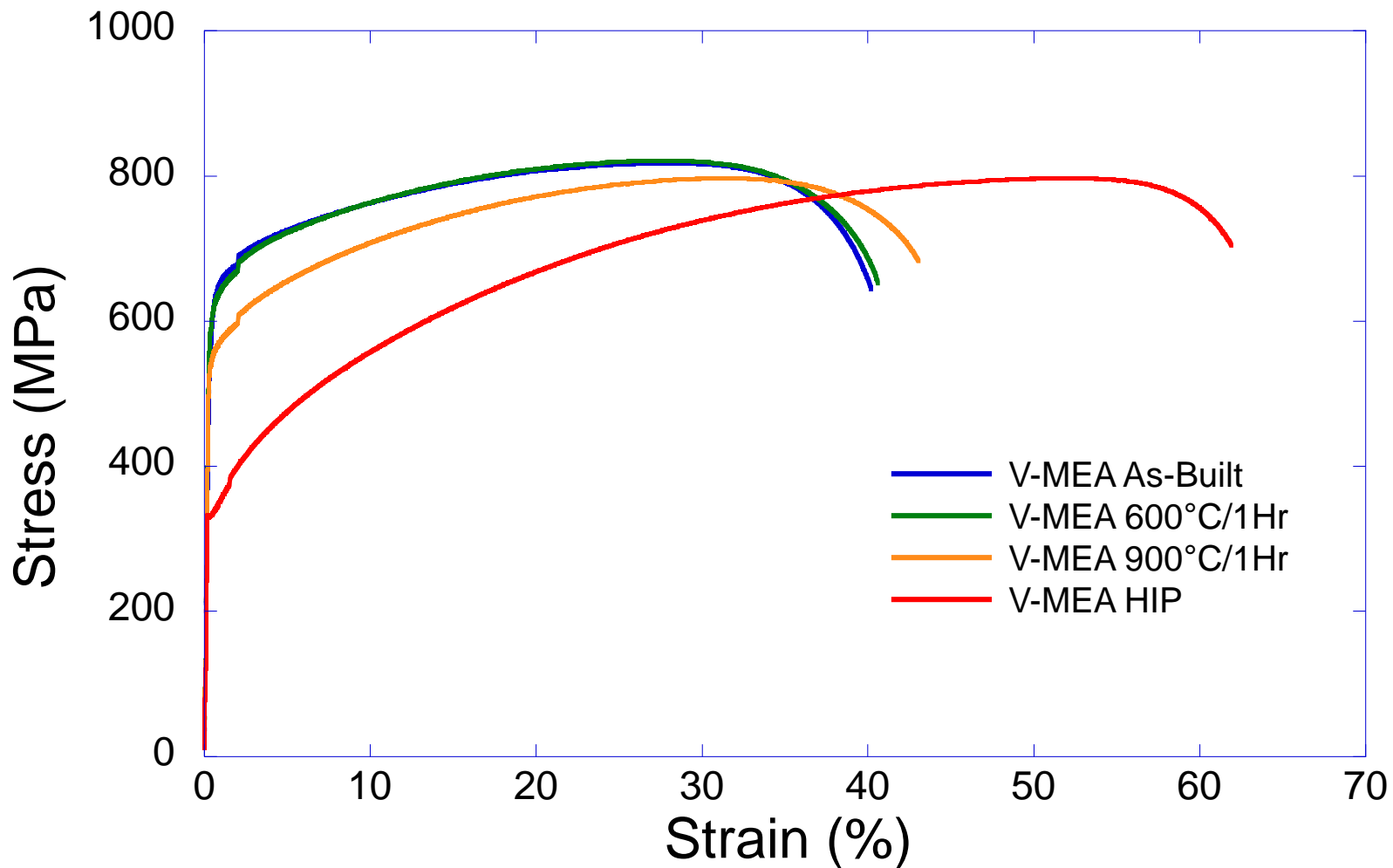
# Microstructure Analysis



- Yttria particles have pinned the grain boundaries in the MEA-ODS builds
- The HIP cycle successfully removed residual stresses in both the V-MEA and DS-MEA builds

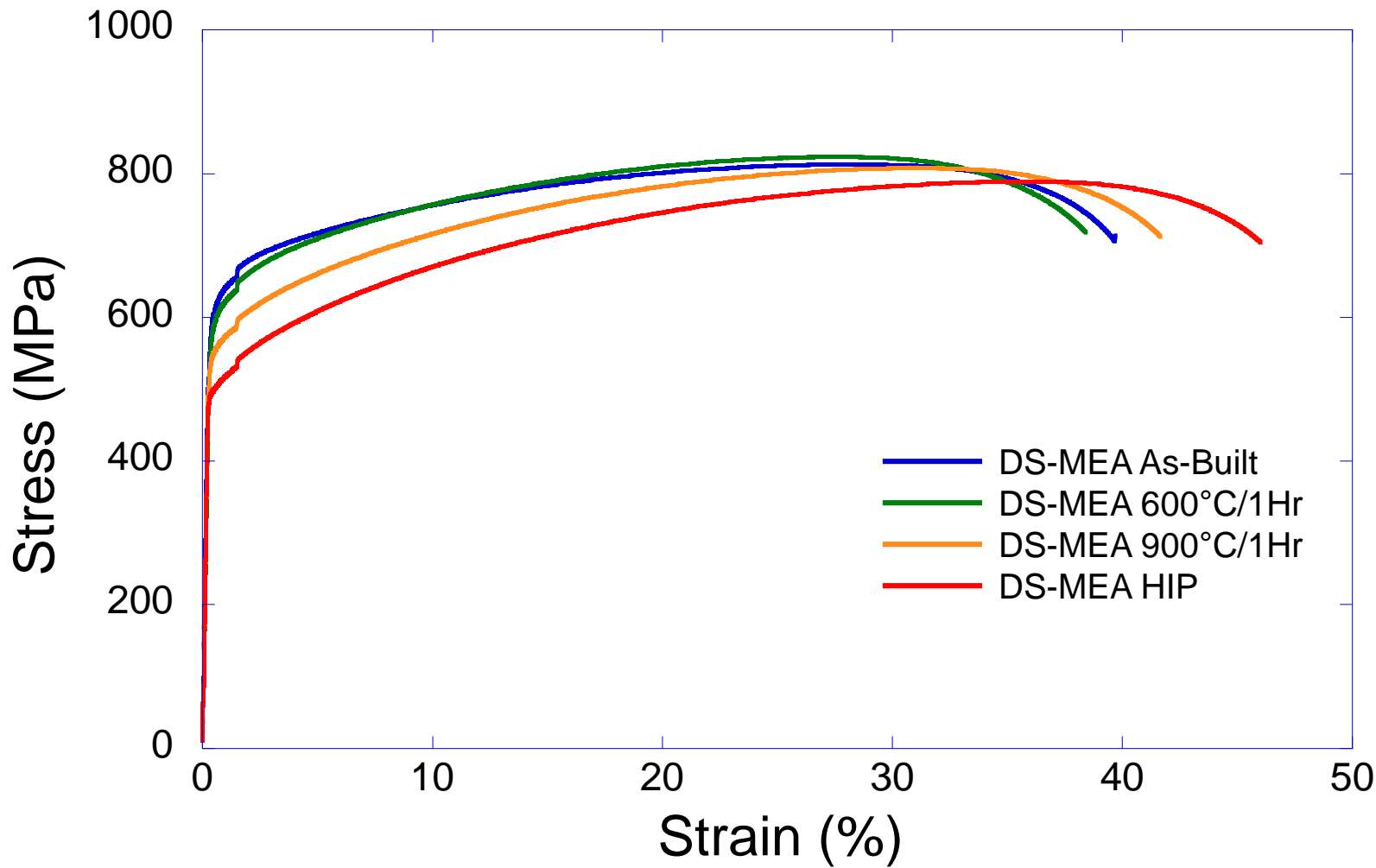


# Mechanical Tests V-MEA



Significant reduction in yield strength associated with experience of extreme temperature for V-HEA specimen

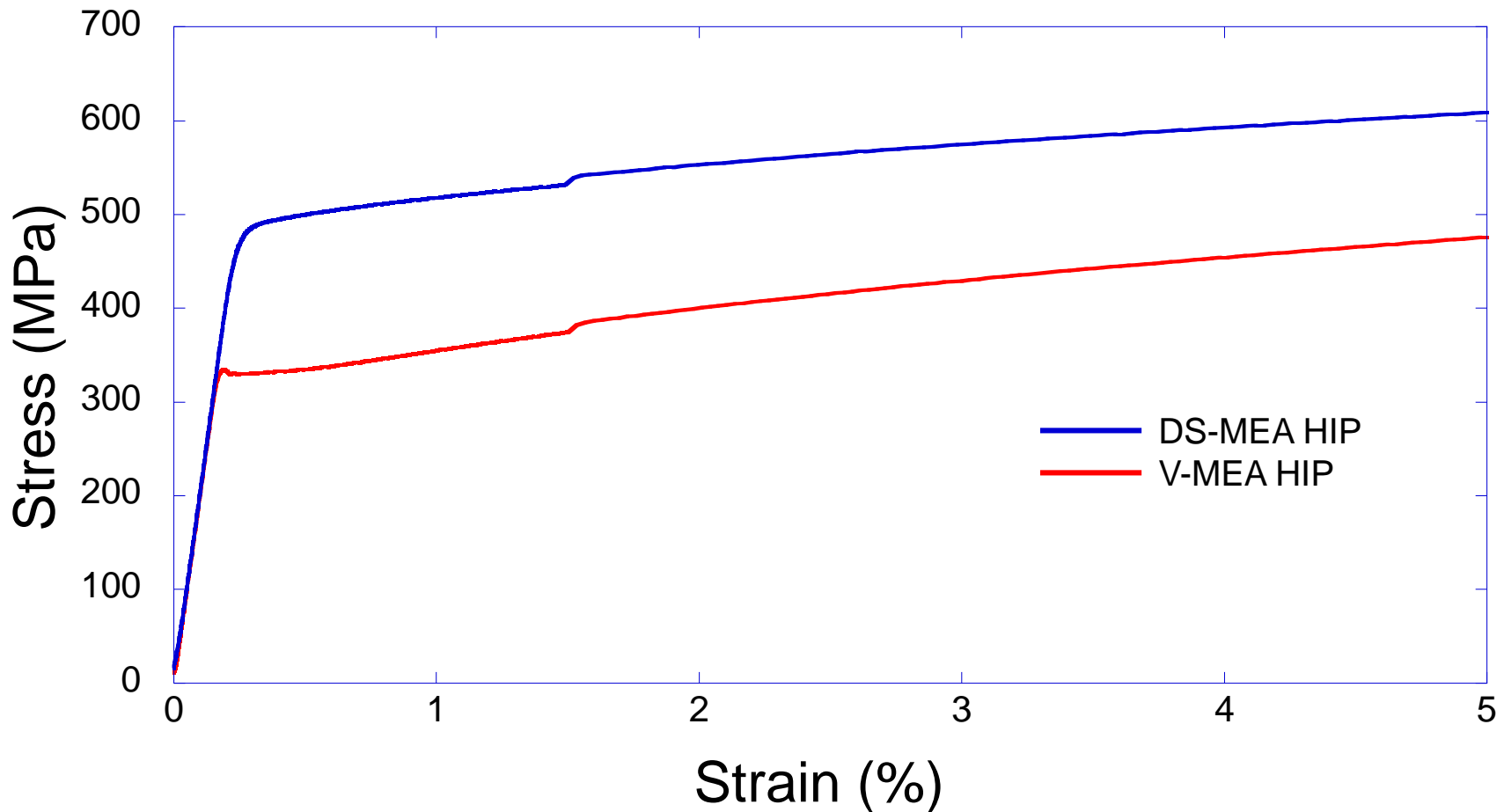
# Mechanical Tests DS-MEA



DS-MEA specimen much less sensitive to extreme environments.



# Yield Strength Curve Comparison



DS-MEA specimen exhibited 50% improvement in yield strength over V-MEA after HIP.



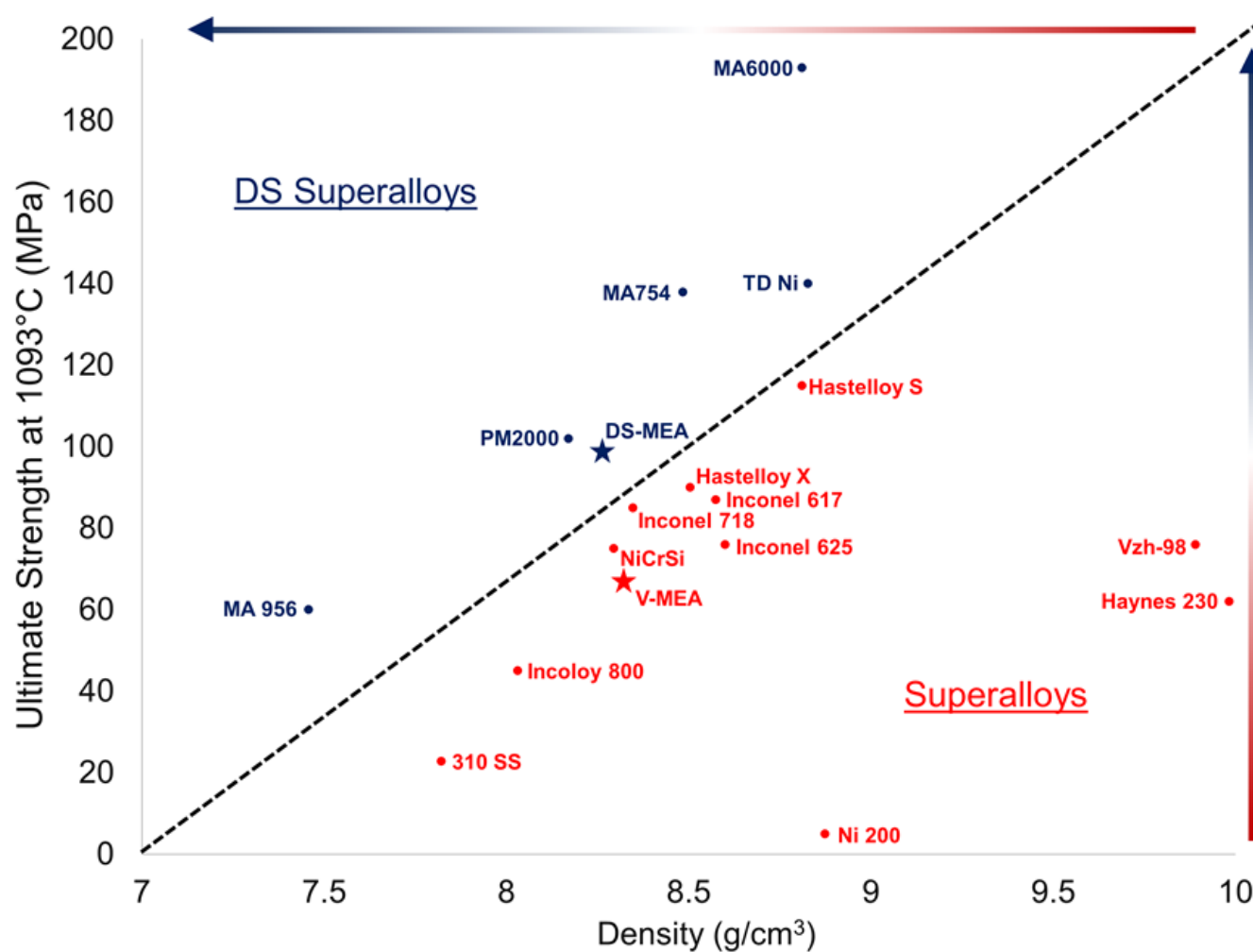
# 1093°C Mechanical Properties

Alloy	Yield Strength (MPa)	Ultimate Strength (MPa)	Elongation (%)	Reduction of Area (%)
V-MEA As-Built	52	68	6.5	7
V-MEA HIP	46	68	8	8.5
DS-MEA As-Built	71	96	20	22
DS-MEA HIP	66	90	19	27

DS-MEA alloys possessed significantly improved high temperature properties over the baseline V-MEA samples.

This includes a >40% increase in strength and a 3x improvement in ductility

# Tensile Strength vs Density Comparison



Scatter plot confirms the successful production of a DS alloy using AM



# Conclusions

- SLM can be leveraged to economically produce dispersion strengthened alloys that until now had been cost prohibitive.
- Multi-principle elements alloys show promise as AM compatible materials
- The incorporation of oxides into the MEA produced a more thermally stable microstructure.
- The DS alloy exhibited improved mechanical properties over the baseline alloy.
- We believe this new manufacturing technique combined with MPEAs opens up a new alloy design space for future high temperature alloys



# Acknowledgments

## Questions?



- ASG
- Dave Ellis
- Henry de Groh
- Quynhgiao Nguyen
- Joy Buehler
- Bob Carter
- Pete Bonacuse
- David Scannapieco
- Cheryl Bowman



# Acknowledgments